Southeastern Geology: Volume 48, No. 4 February 2012

Editor in Chief: S. Duncan Heron, Jr.

Abstract

Academic journal published quarterly by the Department of Geology, Duke University.

SOUTHEASTERN GEOLOGY

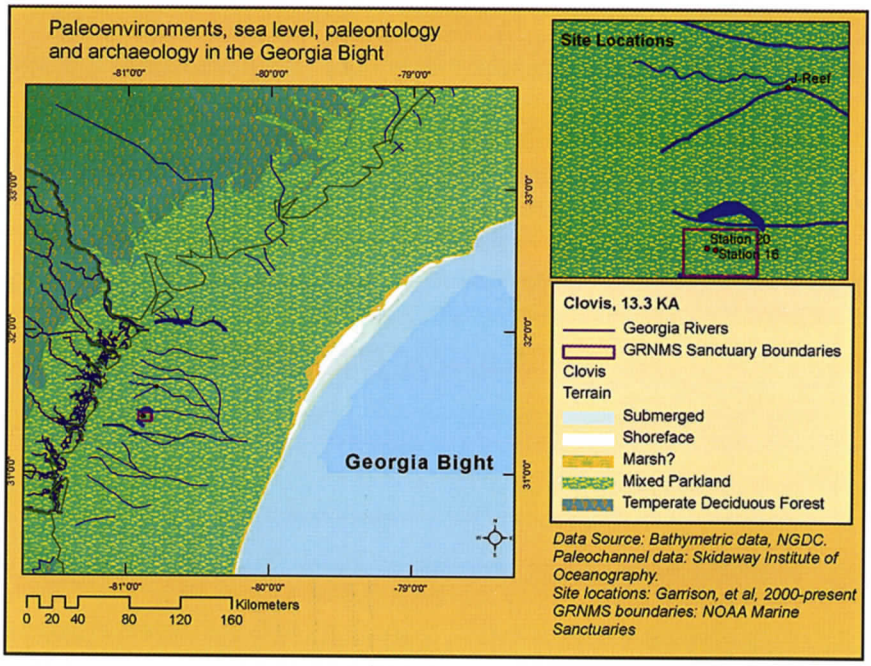

Vol. 48, No. 4 February 2012

SOUTHEASTERN GEOLOGY

PUBLISHED

at

UNIVERSITY OF WEST GEORGIA

This journal publishes the results of original research on all phases of geology, geophysics, geochemistry and environmental geology as related to the Southeast. Send manuscripts to **David Bush, Department of Geosciences, University of West Georgia, Carrollton, Georgia 30118, for Fed-X, etc. 1601 Maple St.,** Phone: 678-839-4057, Fax: 678-839-4071, Email: dbush@westga.edu. Please observe the following:

1) Type the manuscript with double space lines and submit in duplicate, or submit as an Acrobat file attached to an email.
2) Cite references and prepare bibliographic lists in accordance with the method found within the pages of this journal. Data citations examples can be found at http://www.geoinfo.org/TFGeosciData.htm
3) Submit line drawings and complex tables reduced to final publication size (no bigger than 8 x 5 3/8 inches).
4) Make certain that all photographs are sharp, clear, and of good contrast.
5) Stratigraphic terminology should abide by the North American Stratigraphic Code (American Association Petroleum Geologists Bulletin, v. 67, p. 841-875).
6) Email Acrobat (pdf) submissions are encouraged.

Subscriptions to *Southeastern Geology* for volume 48 are: individuals - $27.00 (paid by personal check); corporations and libraries - $44.00; foreign $60. Inquiries should be sent to: **SOUTHEASTERN GEOLOGY, UNIVERSITY OF WEST GEORGIA, DEPARTMENT OF GEOSCIENCES, 1601 MAPLE STREET, CARROLLTON, GA 30118-0001**. Make checks payable to: *Southeastern Geology*.

Information about **SOUTHEASTERN GEOLOGY** is on the World Wide Web including a searchable author-title index 1958-2010 (Acrobat format). The URL for the Web site is: http://www.southeasterngeology.org

SOUTHEASTERN GEOLOGY is a peer review journal.

ISSN 0038-3678

SOUTHEASTERN GEOLOGY

Table of Contents

Volume 48, No. 4 February 2012

SOUTHEASTERN GEOLOGY
V. 48, No. 4, February 2012, p. 165-184

LATE QUATERNARY PALEOECOLOGY AND HEINRICH EVENTS AT GRAY'S REEF NATIONAL MARINE SANCTUARY, SOUTH ATLANTIC BIGHT, GEORGIA

ERVAN G. GARRISON[1], WENDY WEAVER[3], SHERRI L. LITTMAN[2], JESSICA COOK HALE[1] AND PRADEEP SRIVASTAVA[4]

[1]Departments of Geology, Anthropology, University of Georgia; [2]Science Applications International, Inc.; [3]U.S. Army Corps of Engineers, Jacksonville District; [4]Physical Research Laboratory, Earth Science Division, Navrangpura. Ahmedabad, 380 009, India

ABSTRACT

The use of palynofacies as a conceptual tool for the study of depositional environments augments and extends the point-source studies using geophysical, lithological correlation and microfossil analyses of sediment cores in the offshore. We present a synthesis of palynofacies research in the South Atlantic Bight/Georgia Bight, USA. Two research localities - Gray's Reef National Marine Sanctuary (GRNMS) and nearby J-Reef - on the same (-20 m) isobath and only 16 km distant form one another, were characterized in our study. Vibracores to over 4 m below the sea floor were taken at both locations together with hand cores. Outcrops and seafloor exposures were hand sampled. These data are varied and, synthesized elsewhere, yielded insights into the Quaternary paleoenvironments of the coastal plain. Nearshore marine, barrier-back barrier, estuarine-marsh and upland biota provide geologic and ecologic proxies in the form of micro and macrobotanical remains - to include pollen, spores, diatoms, foraminifera and wood. The use of several techniques, notably optical stimulated luminescence (OSL), accelerator mass spectroscopic-radiocarbon (AMS-RC), amino acid racemization (AAR), and uranium series dating methods) has produced a presumptive chronostratigraphy that extends from the Holocene to oxygen isotope stage (M.I.S.) 5. Models based on our pollen results are compared to others proposed for the Mid-Atlantic and Southeast Atlantic regions of the Atlantic coastal plain. Analyses–sedimentological, geophysical, paleoecological and chronological—in the area of Gray's Reef National Marine Sanctuary (GRNMS), have increased our understanding of the late Pleistocene paleoecology and that of relative sea level (RSL) for the now drowned Atlantic Coastal Plain. Palynological data provide a clearer picture of the ecology of the Atlantic Coastal Plain in the latter Pleistocene Epoch, M.I.S.5 through and post-Last Glacial Maximum (LGM / M.I.S.2/ Holocene). Arboreal species, notably oak and pine, dominate the pollen spectra and show clear climate-related variability most notably with Heinrich Events.

INTRODUCTION AND RESEARCH OBJECTIVES

Using Gray's Reef (a National Marine Sanctuary since 1968) and nearby J-Reef, as our study sites, we have collected and examined geophysical, sedimentological, palynological and chronological data for the late Cenozoic - Pliocene and Quaternary - geology of the Georgia Bight (Fig. 1). Our research objectives were to relate our findings to other studies of the east coast as well as to larger issues of paleoclimate, paleoecology and relative sea level (RSL) for the late Cenozoic. In this paper we relate the results of a study of pollen, principally from two sediment cores, to late Pleistocene climate and ecology for the North American southeast, specifically what is today, Georgia, South Carolina and north Florida. A chronostratigraphy, developed simultaneously provides a putative temporal context for the observed variability in both terrestrial arboreal and non-arboreal taxa. These are treated as proxies for paleoclimate and plant ecosystems in the American Southeast (Russell, *et al*, 2009). Our research was undertaken to address those areas where knowledge of the Georgia Bight's Quaternary geology and

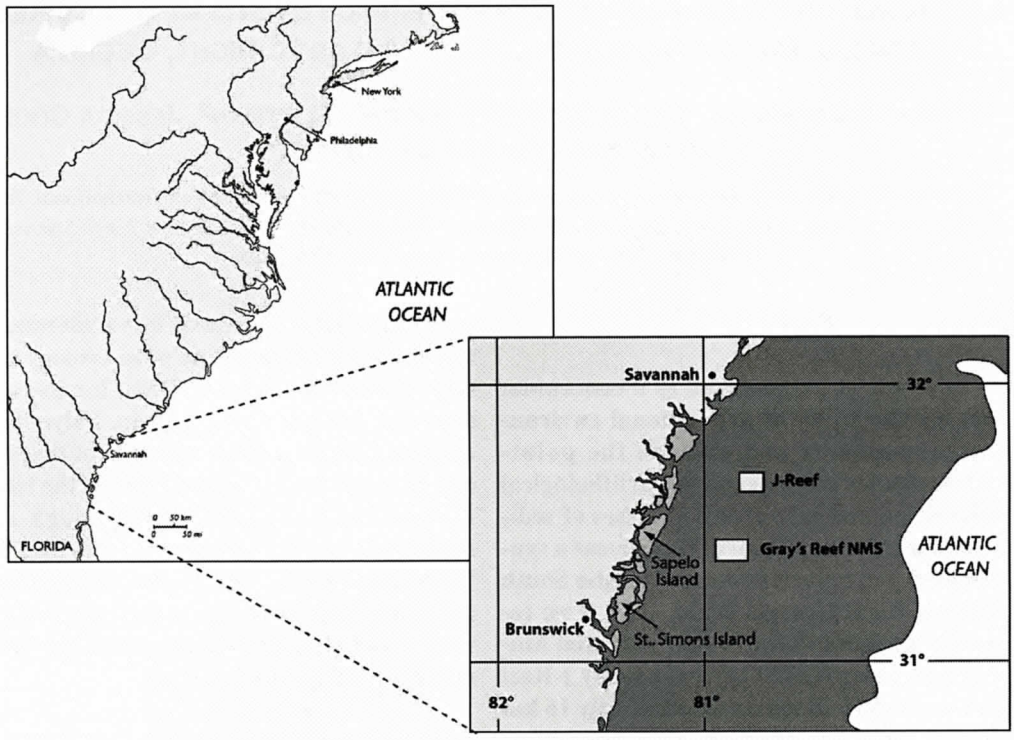

Figure 1. Location map. Gray's Reef National Marine Sanctuary.

paleoecology is not well-developed or is completely unknown. Our results are directly comparative to those of other recent studies for the Middle Atlantic Bight – Virginia and the Chesapeake (Litwin, *et al*, 2010).

Our palynofacies analyses, of sediment facies, at Gray's Reef National Marine Sanctuary (GRNMS), have been carried out on sediment cores - vibracorer and hand - together in tandem with excavated/hand samples from *in situ* outcrops and sea floor exposures. The data for these samples inform us of Pleistocene paleoecology, relative sea level (RSL) and paleoclimate of the now drowned Atlantic Coastal Plain. In particular we present palynological data to provide a clearer picture of the ecology of the Atlantic Coastal Plain in the latter Pleistocene Epoch, M.I.S.5 through and post-Last Glacial Maximum (LGM/M.I.S. 2/Holocene). Using Optical Stimulated Luminescence (OSL), radiocarbon, both conventional and AMS methods, uranium-thorium (U/Th) and Amino Acid Racemization (AAR) dating of sediment cores and shell/wood inclusions, taken in 1996 and 2000, we have produced a presumptive chronostratigraphy that extends from the Holocene to M.I.S. 5.

Arboreal taxa, notably oak and pine, dominate the pollen spectra and previous researchers have shown clear climate-related variability using these taxa (Grimm, *et al*, 1993; Groot, *et al*, 1995; and Markewich, *et al*, 2009). ~~F~~ollowing other workers (Litwin and Andrle, 1992; Grimm, et al, 1993; and Markewich, *et al*. 2009), we use ~~it~~ oak as a *reference taxa* for determining temperate paleoclimate in the South Atlantic Bight coastal region. This variability is to be expected for M.I.S. 3, (60-25 ka), as M.I.S. 3 was a period considered ~~to have been~~ highly unstable, climatologically, with conditions not existing (non-analog) in present-day environments. There seem to have been repeated decadal - scale warming events of 8° – 15° C (Dansgaard-Oeschger (D-O) Events) during this stage (Stewart, 2005; Siddall, *et al*, 2008) With Gonzalez and Dupont (2009) reporting as many as five high-amplitude vegetation shifts during the stage. The timing of excursions, in

the pine-oak ratio, likewise, suggest possible correlations with Heinrich events (HE 2-4) date (Hemmings, 2004; Watts et al. 1992; Grimm, et al, 2006). In conclusion, we will represent our findings in modeled biome maps of the Georgia Bight for selected dates in the late Quaternary in order to graphically illustrate the fluctuations we detect in our data sets.

PHYSIOGRAPHIC AND GEOLOGICAL SETTING

The submerged coastal plain, together with its subaerial component, is covered by Quaternary sediments. Antoine and Henry (1965) described the Quaternary sediments of the Outer Continental Shelf of the Southeastern U.S. as a thin veneer overlying Tertiary bedrock.

The Georgia Bight stratigraphic sequence compresses 2 million years of Quaternary basin-margin evolution into deposits no more than 20 m thick across its breadth. This is a reasonable characterization of the Outer Shelf. The situation of the Inner Shelf is a bit more complex. Quaternary sediments thicken shoreward to 18 meters or more (Woolsey, and Henry, 1974; Woolsey, 1977; Harding and Henry, 1994). Seaward of the modern shoreline Cretaceous-Cenozoic age rocks underlie the Continental Shelf and Slope (Buffler, *et al*, 1978). Current thinking about Quaternary geology in the Southeastern Georgia Embayment/Georgia Bight is found in the comprehensive synthesis by Foyle, *et al* (2004); Foyle and Henry (2004); Huddleston (1988). Pilkey, *et al* (1981) provide an excellent discussion of the offshore geology that compliments Huddleston. Howard, *et al* (1973) provide a representative example of Georgia coastal geology in the context of Chatham County.

Offshore Quaternary and Pliocene units are unconsolidated clastic shallow-neritic sediments - mainly of suborthoquartzitic fine-to-medium-grained sands - overlying a R2 seismic reflector (Foyle, *et al*, 2001). The late Quaternary - Holocene portion of this sand cover is 10-15 m in thickness and rarely goes beyond 15-20 km offshore, pinching out in water depths of 10-15m, (Pilkey and Frankenberg, 1964; Henry and Idris, *supra*) and becoming more coarse-grained. Sexton, *et al* (1992) describe this contact between fine-grained sand and coarser-grained offshore sediments as the outer limit of the zone (modern) of active onshore/offshore sediment transport (Milliman, *et al, supra*; Howard and Reineck, 1972). Some, small, thin patches of fine grained sediment do occur on the inner shelf but the bulk of these sediments occur in drowned stream valleys such as a paleochannel found at J-Reef (Littman, 2000; Garrison, *et al*, 2008).

These sediments have been well described by many workers (Henry and Hoyt, 1967; Millikan, et al 1972; Huddleston, 1988; Swift, *et al* 1972; Swift and Niedorada, 1985). Their nature have been defined on the basis of more than 6000 bottom samples carried out by the Woods Hole Oceanographic Institution (WHOI) and the United States Geological Survey (USGS) prior to 1970 (Milliman, *et al*, supra). Continued coring studies by such workers as Coastal Carolina University (Gayes, *et al* 1992) and the University of Georgia (this study) have provided corroboration and detail to the knowledge of shelf sediments. Based on these and other studies (Idris and Henry, 1995; Henry and Idris, 1992), 10 glacio-eustatic events have been identified (Foyle *et al*, 2004:73). The record of these 10 events, paleoshorelines, submerged or stranded barriers, is extremely incomplete on the shelf of the Georgia Bight (*supra, 73*). These glacio-eustatic events are preserved on the North Carolina shelf in paleochannels (*supra;* Duane, *et al*, 1972).

METHODS

Sediment Coring

A total of 11 vibracores, 7 taken in 1996 and 4 in 2000, (Table 1) were recovered on two cruises on the NOAA Ship *Ferrel*. The data sediment cores were analyzed lithologically and geochemically (Littman, 2000) and then for pollen (Weaver, 2002). The sediment cores, taken in 1996, were retrieved using a 3 inch (7.6 cm) diameter core barrel pneumatic vibracorer provided by Rice University Geosciences De-

Table 1. 1996 and 2000 Vibracore locations at Gray's Reef and J Reef.

Site	Year	Latitude	Longitude	Water depth (m)	Core length (m)
J Reef (A)	(1996)	31°E 35.89'	80°E 47.93'	19.2	1.98
J Reef (B)	(1996)	31°E 35.89'	80°E 47.93	19.2	2.74
Gray's Reef (1)	(1996)	31°E 24.62'	80°E051.2'	19.5	3.66
J Reef (1996)	(1996)	31°E 35.56'	80°E 47.03'	21.	<2
J Reef (4)	(1996)	31°E 35.9'	80°E 47.75'	20.4	4.57
GR1a site (4)	(1996)	31°E 24.616'	80°E.47.100'	17.6	-2.4
GR - NE (3)	(1996)	31°E 24.7'	80°E 50.8'	19.5	2.15
GR-NW(2)	(2000)	31°E 24.381'	80°E 54.267'	16	<1
GR-SW: (3)	(2000)	31°E 22.30	80°E 55.00'	17.3	1.36
GR-SW:(4)	(2000)	31°E 24.646'	80°E 51.194'	19.4	2.35
GR-SW:(5)	(2000)	31°E 22.646'	80°E 51.194'	19.4	2.04

partment. The 2000 cruise used a 3 (7.6 cm) inch diameter core barrel hydraulic vibracorer built by Coastal Carolina University's Institute of Lowland and Coastal Studies. Both vibracoring systems produced continuous sediment cores of 2 – 3+ m lengths. These cores were taken in two locales along or near the –20 m isobath, Gray's Reef and J-Reef (Table 1). Gray's Reef is a series of natural rock outcrop or hard bottom while J Reef is an artificial reef/fish haven made up of scattered patch reefs. Cores were taken at the latter location because of the presence of a drowned paleochannel and incised valley (Garrison, *et al*, 2008).

In addition to the vibracores, sediments were retrieved by use of diver-deployment hand-and-hydraulic corers with1 in (2.54 cm) to 2 in (5.08 cm) diameter barrels. These devices, plus simple hand excavation, were utilized in areas too close to the Gray's Reef outcrop for the use of the larger vessel-deployed systems. Two of these cores were analyzed by Rich and reported in Russell, *et al*, 2009; this paper).

All vibracores were split into working and archival halves. The hand cores were extruded into core trays or split into halves. The 1996 vibracores were logged and photographed along their length. Sediment samples were taken at natural stratigraphic breaks, 5 cm on either side of an observed contact. The cores were sampled for shells and macro-micro paleobotanical (wood/pollen) remains. Shell (*Mercenaria, Astarte*) taken from these cores was utilized in AAR dating studies (Table 2). The 2000 vibracores were logged and photographed as in 1996. In contrast to 1996, due in part to a focus on palynological study, two cores, 3 and 5, were sampled at 10 cm intervals along their length. In both cores, every other sample from top-to-bottom was eliminated yielding a total of 17 sediment samples of 15 cc each (8 from core 3, 9 from core 5). Cores 1 and 2, from 2000, were left unopened. Core 4 was sampled for chronostratigraphy purposes. The working halves of the 1996 cores (GRNMS 1; J Reef 1 & 4) were used for geochemical studies (metal oxides), and organic matter (OM), Loss-on-ignition (LOI). Acid digestion of the carbonate fraction was measured on the Gray's Reef cores. No geochemical studies were made on the 2000 cores. LOI was done and, for the 2000 cores, magnetic susceptibility was measured using a Williams magnetic bridge susceptibility meter. All particle size analyzes were done using the Flealer method (Indurante, *et al.*, 1990). LOI results were used to select cores taken in 2000 that were suitable for pollen studies. Munsell soil color (wet) was recorded for all cores. The geochemical results were reported in Littman's unpublished masters thesis (2000).

Geophysical

The 1996 geophysical study used a Datasonics SBP 5000 seismic profiling system and an EG&G Model 260 side scan sonar. While both side scan sonar (100 kHz) and subbottom seismic reflection (3.5 kHz) data were acquired in the 1996 *Ferrel* cruise, only subbottom (3.5 kHz) data were acquired in a second geophysical cruise in 1998. In 2000, the seismic profiler was used again without concurrent side scan sonar mapping. In 2001, a multi-beam sonar mosaic was made of the sanctuary by the NOAA Ship *Whiting*. The reasons for the focus on seismic data were twofold: (1) the shelf, with exception of the Gray's Reef outcrops are more-or-less featureless sand bottom in the study area and (2) a paleochannel discovered in 1996 was more thoroughly mapped and characterized in 1998. The vertical resolution of the 3.5kHz system, a Datasonics SBP5000, is approximately 1m. Results of these surveys were compared to baseline seismic studies such as those by Henry *et al* (1981) and Henry and Idris (1992).

Palynological and Macrobotanical

Samples for pollen processing were taken from cores 3 and 5 taken in 2000. Since the sediments in both cores contained sand (except for the surface of core 5) and therefore, less organic content, more sediment (10-15 cc) was required to obtain pollen concentrations comparable to the typical 1cc sample of peat or clay. Heusser (1983) and Heusser and Stock (1984) have shown this to be an effective strategy and equivocal to smaller samples collected from peat. The United States Geological Survey (USGS) also recommends the use of larger samples in sandy sediment to obtain a significant number of countable pollen grains (Deb Willard, 2000, personal communication). This technique was confirmed in a previous attempt to extract pollen from a small core taken from Gray's Reef (Littman, 2000; Russell, *et al*, 2009).

The 1996 sediment cores were examined by Rich and Booth and reported in Russell, *et al* (2009). Two of these cores – 1 and 2 (Table 4) - were only sampled in the upper 10-15 cm of the core so only the upper sections of cores 3 and 5 are comparable. The core referenced in Table 4 as "Gray's Reef clay" was bulk sampled within it less than 0.5 m length.

Core 3 pollen samples were collected within 1 cm intervals and contained 10 cc or about 13-15 grams of sediment. Eight samples were taken. All attempts were made to avoid fragments of shell in the collection process and obtain exactly 10 cc of sediment. Core 5 pollen samples were also collected within 1 cm intervals and contained 15cc or about 16-18 grams of sediment. The amount of sediment sampled was adjusted upwards to obtain greater pollen concentration in case core 3 samples failed to yield substantial amounts of counting. No attempt was made to make the surface clay sample from core 5 equivalent to the sand samples to adjust for pollen density. All attempts were made to avoid fragments of shell in the collection process and obtain exactly 15cc of sediment. Core 5 produced 9 samples that were selected on the basis of higher organic content and relevant spacing in the core.

Pollen processing was conducted according to Shane (1992) and Heusser and Stock (1984). *Eucalyptus* spike was used as exotic marker pollen and standardized according to Shane (*supra*). Both core 3 and core 5 samples received 5 ml of *Eucalyptus* spike. Processing involved the use of hot 10% KOH to remove organic acids. After sieving through 180 micron mesh to remove sand, the samples were treated with hot 10% HCI and concentrated HF to remove inorganics and silicates. Acetolysis removed remaining organics and then stained the pollen grains. Pollen was then mounted in silicone oil for viewing.

Pollen slides were counted along systematic transects at 400x magnification. A minimum of 300 pollen grains per sample interval were counted. Unknown, indeterminate (crumpled and deteriorated), and *Eucalyptus* pollen grains were also counted. Number of slides per sample interval ranged from 1.5 to 7 to achieve a total of 300 grains of pollen per interval. Identification of the pollen taxa to family or genus was based on the reference collection at the University of Georgia Paleoecology Laboratory.

Table 2. Chronology of Sediments at Gray's Reef and J-Reef[a]

Method	Sediment	Material	Location	Laboratory	Age ^{14}C Yr BP[b]	Age cal yr BP[c]	Age OSL / U/Th Yr BP
AMS	Gray Shelly Sand	Bone	Surface Sediment[d]	Beta-103683	6090+/-60	7160-6790	
AMS	Gray Shelly Sand	Shell	Surface Sediment[d]	UGA-11688	8950+/-70		
AMS	Gray Shelly Sand	Carbonate	Surface, (*Ophimorpha*)[d]	Beta-92356	18970+/-140	22479-20571	
OSL	Gray Shelly Sand	Quartz Sand	Core 4, -30/cm[d]				24023+/-4954
AMS	Gray Shelly Sand	Shell	Core 4, -30/cm[d]	Beta-172381	29120+/-690		
AMS	Gray Shelly Sand	Shell	Core 4, -170/cm[d]	Beta-172380	24640+/-460		
OSL	Gray Shelly Sand	Quartz Sand	Core 4, -170/cm[d]				23702+/-5411
AMS	Gray Shelly Sand	Shell	Core 1, -170/cm[d]	UGA-11689	43770+/-470		
OSL	Brown Sand	Quartz Sand	Core 1, -220/cm[d]				39265+/-5692
U/TH	Brown Sand	Sediment	Core 1, -220/cm[d]				37481+/-1372
AMS	Gray Shelly Sand	Shell	Reef Front, -15/cm[d]	UGA-11690	45170+/-1530		
AMS	Gray Mud	Wood (*Taxodium*?)	Core 1, -220/cm [e]	Beta-103780	>50290		
AMS	Gray Mud	Wood	Core 4, -220/cm [e]	Beta-105507	>48020		
AMS	Brown Sand	Oyster Shell	Reef Front, ~10 cm [e]	UGA-00887	31082+/-180		
AMS	Brown Sand	Scallop Shell	Reef Front, ~10 cm [e]	UGA-00888	35055+/-248		
AMS	Gray Shelly Sand	Wood	Reef Front, ~10 cm [e]	UGA-01045	35767+/-264		
AMS	Gray Shelly Sand	Wood	Reef Front, ~10 cm [e]	UGA-01046	39316+/-316		
AMS	Concreted Shelly Sand	Scallop Shell	Reef Front, ~10 cm [e]	UGA-00889	421496+/-396		
AMS	Gray Shelly Sand	Wood (*Licaria* sp.)	Reef Front, ~10 cm [e]	UGA-00782	41326+/-455		
AMS	Gray Shelly Sand	Wood (*Juniper* sp.)	Reef Front, ~10 cm [e]	UGA-00890	40488+/-350		
AAR	Gray Shelly Sand	Mercenaria	Grays Reef	jw2009-018-001		MIS 5	
AAR	Gray Shelly Sand	Mercenaria	Grays Reef	jw2009-018-000	47900+/-560	MIS3	
AAR	Gray Shelly Sand	Mercenaria	Grays Reef	jw2009-018-005	47900+/-610	MIS 3	

Differences in preservation of pollen can bias interpretation. The substance in the outer covering (exine) of the pollen grain, sporopollenin, is variously resistant to decay, depending on the species. Pine (*Pinus*) pollen is the more resistant, while maple (*Acer*) is very susceptible to decay. Oak is a resistant pollen type. Production of pollen is also variable between species. A single pine tree produces about 10 billion grains per year. *Artemsia* species are, likewise, high pollen producers and represent 40-50% of the pollen spectra in some plant communities (van Geel and Dirkesen, 2006). Hence, species may be either over-represented or under-represented in the pollen record.

Mode of dispersion also determines representation in the pollen record. Pollen transported via wind tends to be over-represented, as grains of pine and *Ephedra* can be found hundreds of kilometers from where they grow. Pine pollen has even been found in the Arctic. Animal transport tends to under-represent pollen with dispersal distance only a few meters. In the marine environment the dispersal of pollen can occur one of two ways or both – aeolian and waterborne. From M.I.S. 5 (ca. 125 ka) to mid-M.I.S. 3 (ca. 45 ka) the latter dispersal mode dominated in the area of Gray's Reef. After that time, until the early-to- mid-Holocene, the aeolian mode dominated over a subaerial coastal plain.

Studies of pollen found in marginal marine and marine epicontinental deposits have examined both modes of dispersal and preservation (Pieñkowski and Wakmundzka, 2009; Williams, *et al*, 1995). Typically, the transport paths for pollen begin with aeolian dispersal into a marine environment becoming waterborne thereafter. Such dispersal can lead to the extra-local deposition of "exotic" pollens much like that of the pine example for the Arctic.

Bissacate pollen grains, produced by conifers, as well as some other arboreal species, have air sacs which assure wider dispersal of this grain type as opposed to monosulcate varieties (Pieñkowski and Wakmundzka, 2009. Likewise, sporomorphs tend to be less frequent in marine environments because they are more easily destroyed by waves and currents. Arboreal pollen, notably, the bissacate species, increase in proportion to other taxa, becoming preferentially concentrated in offshore deposits.

Surprisingly enough, our surveys at both Gray's Reef and J-Reef recovered wood on the seafloor and shallowly buried in the sediment outcrops. A relatively intact *Licaria triandra* (Pepperleaf sweetwood) sample was recovered, identified and dated (see Table 2) as was a sample of *Juniperis* (red cedar) also identified and dated. An *Abies* cone was found at J-Reef, which dated to the present day. A fragment of *Fagus* was found in a J-Reef core. The exact genus remains to be determined for this find. While not enough macrobotanical material to allow speculation on the species composition of a M.I.S. 3 forest, none of these genera are out-of-place in Southeastern arboreal communities of that time albeit the modern range, today, for *Licaria* does not extend beyond south Florida (Richter, 1985). Certainly, based upon our findings, the coniferous macrobotanical material is consistent with the palynological data shown in Table 3.

The beech, cedar and bay families, represented in the macrobotanical remains, were all identified on the basis of wood architecture by the U.S. Department of Agriculture Wood Identification Laboratory located at the

[a]The chronostratigraphic zones correspond to lithostratigraphic levels: 6 000 YBP to 18 000 YBP, surface sediment, Gray Shelly-Sand; 23 000 YBP to 28 000 YBP, Concreted Shelly-Sand and Gray laminated mud; 39 000 YBP to >50 000 YBP, Brown Sand 31 000 YBP 38 000 YBP. The dates for wood inclusions found in the Gray Shelly-Sand are assignable to the Concreted Shelly-Sand which is their place of origin.
[b]Conventional radiocarbon age, $\delta^{13}C$ corrected using the Libby14 (half-life 5568 years). Errors represent 1 standard deviation.
[c]Calibrated radiocarbon age in years before A.D. 1950. Based on INTCAL98 calibration data using CALIB 5.01 (Stuiver, et al 1998). Calibration done only for ages <20,26514 C yr. B.P. Range represents 1 standard deviation.
[d]Sample located at Grays Reef

Table 3a. Pollen species and counts, core 3, Gray's Reef

Taxa	3 cm	21 cm	41 cm	57 cm	81 cm	99 cm	121 cm	134 cm
Pinus	237(75)	227(76)	238(76)	253(84)	247(82)	225(75)	228(76)	259(86)
Picea	0	0	0	0	0	0	0	0
Taxodium/Juniperus	7	1	0	3	3	0	1	0
Quercus	54(17)	45(15)	32(10)	30(10)	47(16)	48(16)	54(18)	12(4)
Nyssa	3	0	0	0	0	1	0	0
Alnus	0	0	0	1	0	1	0	0
Liquidambar sp.	0	5	7	5	6	6	6	4
Betula	1	1	1	2	6	2	4	0
Carpinus/Ostyra	8	1	2	1	0	2	0	1
Corylus	0	0	0	0	0	0	0	0
Carya	0	0	2	1	0	1	4	1
Ulmus	0	0	2	1	2	0	0	0
Lirodendron tulipfera	0	0	0	1	0	0	0	0
Fagus	0	0	16(5)	6(2)	0	6(2)	2	0
Salix	0	0	0	0	0	1	0	0
Fraxinus	0	0	0	0	0	0	0	0
Castanea	0	0	1	0	0	1	0	0
Myrica	0	0	0	0	0	0	0	0
Ilex	0	0	0	0	0	0	0	0
Smilax	0	0	0	1	0	0	0	0
Graminae	0	0	0	0	0	0	0	0
Ambrosia type	5	1	2	1	5	3	5	1
Artemesia	0	0	0	0	0	1	0	0
Chenopodieae	11	0	4	2	3	1	1	0
Plantago	0	0	0	0	0	0	0	0
Lycopodium	0	0	0	0	0	0	0	0
Osmunda	0	0	0	0	0	0	1	0
Sphagnum	0	0	0	0	0	0	0	0
Sagittaria	0	0	0	0	0	0	0	0
Myriophyllum	0	0	0	0	0	0	0	0
Typha	0	0	0	1	0	0	0	1
Unknown and Indeterminate	9	11	37	32	18	29	10	21

Percentages are shown, in parentheses, for selected taxa for a better comparison with those same taxa shown in Table 4.

Table 3b. Pollen species and counts, core 5, Gray's Reef

Taxa	surface	11 cm	21 cm	31 cm	71 cm	111 cm	151 cm	171 cm	198 cm
Pinus	198(63)	225(73)	233(75)	250(81)	246(79)	240(77)	245(79)	273(88)	267(86)
Picea	0	0	0	0	0	0	1	0	0
Taxodium/Juniperus	4	8	2	0	1	0	0	0	0
Quercus	56(18)	38(12)	46(15)	36(12)	34(11)	32(10)	41(13)	15(5)	50(16)
Nyssa	0	0	0	1	0	0	2	0	1
Alnus	1	0	0	0	0	0	0	0	1
Liquidambar sp.	8(3)	9(3)	2	7(3)	7(3)	7(30	5	5	5
Betula	5(2)	2	1	1	1	2	1	2	5(2)
Carpinus/ Ostyra	1	0	1	2	2	2	3	0	0
Corylus	0	0	0	0	0	0	0	0	0
Carya	1	0	3	0	2	2	4	2	0
Ulmus	2	0	0	1	1	1	0	0	0
Lirodendron tul	2	0	0	0	0	0	0	0	0
Fagus	1	1	0	1	0	0	1	1	3(<1)
Salix	1	0	0	0	0	0	0	0	0
Fraxinus	0	0	0	0	0	0	0	0	0
Acer	2	0	0	0	0	0	0	0	0
Castanea	0	0	0	0	0	0	0	0	0
Myrica	0	0	0	0	0	0	0	0	0
Ilex	1	0	0	0	0	0	0	0	0
Smilax	0	0	0	0	0	0	0	0	0
Graminae	0	0	0	0	0	0	0	0	0
Ambrosia type	5	1	3	3	2	0	2	2	0
Artemesia	0	1	1	0	0	0	0	0	0
Chenopodieae	2	4	2	3	2	0	1	0	0
Plantago	0	0	0	0	0	0	0	0	0
Lycopodium	1	0	0	0	0	0	0	0	0
Osmunda	0	0	0	0	0	0	0	0	0
Sphagnum	0	0	0	0	0	0	0	0	0
Sagittaria	0	0	0	0	0	0	0	0	0
Myriophyllum	0	0	1	1	1	0	0	0	0
Typha	0	0	0	0	1	0	0	0	0
Unknown and Indeterminate	30	22	20	17	13	19	18	9	28

Percentages are shown, in parentheses, for selected taxa for a better comparison with those same taxa shown in Table 4.

University of Wisconsin. The fir was identified by it seed cone. Most of the specimens showed some marine borer damage but were surprisingly intact with some encrusting. The *Licaria* find was freeze-dried when first recovered but simple air drying was sufficient for the remainder of the finds.

Geochronological

The chronology of the cores are based on conventional/accelerator mass spectrometry (AMS) radio-carbon dates (6); optical stimulated luminescence (OSL) dates (3) and one uranium-thorium (U/Th) age. The AMS ages were determined from a variety of material found in the cores or in excavation - bone, shell, carbonate and wood. The OSL and U/Th ages were derived from sediments taken from cores. The radiocarbon laboratories used in this study were Beta Analytic Incorporated (BETA), Miami, Florida; The University of Georgia Center for Applied Isotope Studies (UGA). All samples were thoroughly pre-treated with standard acid-alkali-acid washes prior to isotopic analysis by accelerator mass spectrometry (AMS).

Optically stimulated luminescence (OSL) dating was carried out under controlled red-light conditions in the laboratory. The samples were treated with 10% HCl and 30% H_2O_2 to remove carbonates and organic material and sieved to obtain the 120-150μm size faction. Na-Polytungstate ($\rho = 2.58$ g/cm^3) was used to achieve density separation of quartz and feldspar minerals. The quartz fraction was then etched with 40% HF for 80 min followed by 12N HCl for 30 min to remove the alpha skin. Separated quartz grains were mounted on stainless steel discs with help of *Silkospray*™. Light stimulation on quartz mineral extracts was done using a Risr array of combined blue LEDs centered at 470nm. Detection optics comprised Hoya 2×U340 and Schott BG-39 filters coupled to an EMI 9635 QA Photomultiplier tube. Measurements were made using a Risr TL-DA-15 reader. A 25 mCi $^{90}Sr/^{90}Y$ built-in source was used for β-irradiation. U and Th for dose rate calculation were estimated using a thick source Daybreak alpha counting system. K was estimated through ICP-MS using the fusion technique for total K extraction at the XRAL laboratory in Toronto, Canada.

The SAR protocol (Murray and Wintle, 2000) was used to determine the paleodose. A five-point measurement strategy was adopted with three dose points to bracket the paleodose, fourth zero dose and fifth a repeat-dose point. Repeat dose was measured to correct for sensitivity changes and to ensure that the procedure was working correctly. All measurements were done using a preheat of 220°C for 10s followed by OSL sampling carried out at 125°C for 100s. For all aliquots the recycling ratio between the first and the fifth point was ranged within 0.95-1.05. Data were analyzed using ANALYST software (Duller, *et al*, 1999).

The U/Th age was determined by gamma counting the reef sediment with inductively coupled plasma - mass spectrometry (ICP-MS). Uranium activity/amount was determined using the isotope Pa-234m while thorium was estimated using the isotopes Bi-214 and Pb-214. The radiocarbon ages are conventional ages, corrected to the $^{13}C/^{12}C$ ratio, and use the Libby ^{14}C half-life of 5568years. Calibrated ages are given in years before A.D. 1950 while those of OSL are reported as years before A.D. 2003 when the OSL paleodoses were determined. The U/Th age is reported as years before A.D. 1950.

Groot, *et al* (1995) combined palynological studies of sediment cores from the Atlantic continental shelf with amino acid racemization (AAR) analyses. In our study we have used racemization dating of specimens of *Mercenaria* and *Astarte* from both cores and the sea floor deposits. These results were obtained using gas chromatography to assess the amounts of eight amino acids (Wehmiller, 2010). *Mercenaria* sections, weighing ~ 0.1 to 0.4 g were cut from whole or partial shells. These samples were mechanically cleaned then alternately rinsed with 2N HCL and distilled water for a final hydrolysis satge at 6N HCL at 105° C for 22 hours. Analyses were then done using a 25 m Chirasil-val® gas chromatographic Column installed in an Agilent® gas chromatograph equipped with both flame ionization (FID) and nitrogen-phos-

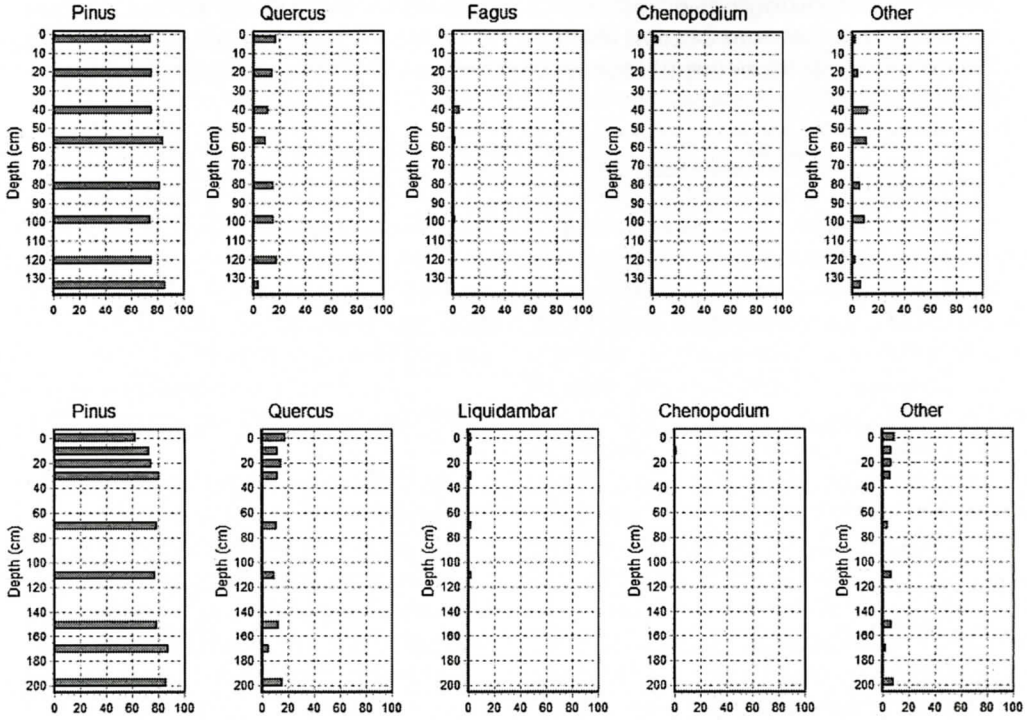

Figure 2. Histogram plots of pollen from Gray's Reef (2000) sediment cores 3 (upper) and 5 (lower). *Fagus* was not observed in core 5 whereas *Liquidambar* was observed in 5 but not in core 3 (cf. Table 3).

phorous (NPD) detectors. Precision of D/L values for multiple derivative samples are better than 2%. Analytical results are managed in a database maintained by the University of Delaware's Department of Geological Sciences.

The amino acid racemization (AAR) dates (Table 2) are preliminary, with only three samples dated, all of clam species, *Mercenaria*. The dates for these samples range from M.I.S.5 (2) to M.I.S. 3(1) (John Wehmiller, Personal Communication, 2009). The latter was confirmed by AMS dating.

RESULTS AND DISCUSSION

Our paleoecological data provide corroborative support for a lithostratigraphic- chronostratigraphic sequence in the late Pleistocene that more clearly delimits floral communities in M.I.S. 3/2. We have emphasized palynological data in this study.

Grimm, *et al* (1993), in a study of a 18.52 m core from Lake Tulane (Florida) specifically linked pine:oak-*ambrosia* pollen abundance to climatic oscillations. That study linked these oscillations to massive, periodic advances of ice streams from the Laurentide ice sheet (L.I.S.) margin (Heinrich Events (H.E.)(Hemmings, 2004). Their conclusions were that there were frequent, major vegetation shifts from pine forest to open oak-savanna/grassland over the late Quaternary (<50 ka). In the 1993 paper, Grimm *et al*, argued that pine signaled a cooler climate. In 2006, Grimm, *et al*, reinterpret the Lake Tulane data such that peaks in the pine pollen are, indeed, linked to Heinrich events but do not necessarily imply a cooler climate. In this later study, Grimm, *et al*, suggest a wetter, warmer climate associated with peaks in pine. Oak pollen, by contrast, signal a somewhat cooler climate for Florida in the late Quaternary. Watts *et al* (1992) conclude that the late MIS 3 is a peri-

Table 4. Palynological composition of samples from Gray's Reef. Values are expressed as percent of total identifiable pollen and spores (minimum number of 300 grains: F. J. Rich, unpublished data (in Russell, 2009; see Table 1 for these core locations)

Taxon	Gray's Reef clay	Gray's Reef core 1	Gray's Reef core 2
Alnus	2.3	1.3	2.1
Ambrosia	0.89	0.97	0.62
Asteroideae	1.5	–	–
Betula	0.59	0.97	0.98
Carya	3.6	1.9	1.2
Castanea	0.29	1.6	0.62
Chenopodiaceae/Amaranthaceae	15.2	8.1	5.6
Corylus	0.32	0.62	–
Cyperaceae	1.2	0.32	–
Fagus	0.59	0.32	–
Fraxinus	0.29	0.32	0.62
Gramineae	2.7	6.8	0.98
Iva	0.59	0.65	–
Liquidambar	1.8	–	0.30
Myrica	1.2	0.32	0.30
Osmunda	0.59	0.32	–
Ostrya/Carpinus	–	0.32	–
Picea	2.1	–	–
Pinus	41.7	56.5	67.2
Polygonum	0.59	–	–
Polypodium	–	0.65	–
Pteridium	–	0.32	–
Quercus	13.4	12.7	13
Salix	0.59	–	0.62
Sambucus	–	0.32	–
Sphagnum	0.29	0.32	–
Stellaria	0.29	–	–
Taxodium	2.1	–	–
Tsuga	0.59	–	–
Ulmus	0.59	0.97	0.62
Woodwardia	2.1	0.97	–
Indeterminate	2.1	2.6	3.7
Totals	100	100	99.4

od of unstable climate with little or no homogeneity over many thousands of years. Their conclusions are based on data for northwest Florida (Camel Lake and Sheelar Lake) where a species-poor pine forest, with some oak, existed. A cursory inspection of Table 3/Figure 2 shows the dominance of pine and oak at Gray's Reef during this same interval. Likewise, there are two significant pine:oak ratios shifts in the Gray's Reef pollen (-134 cm, core 3; -171 cm, core 5). In both cases the oak percentage drops to 5% or less. The increase in pine is not as dramatic but significant nonetheless.

Two salient points can be made from these results:

(1) Palynological studies of pollen from marine sediments have a demonstrated utility in discussions concerning the reconstruction of paleoenvironments, and,

(2) Oscillations in arboreal pollen spectra, particularly that of pine:oak, can be linked to climatic shifts, at a millennial or higher resolution scales.

Palynological studies of marine sediments, therefore, from both Gray's Reef have allowed us to gain a broad-brush picture of past environments on the Quaternary coastal plain and correlate this to changes in paleoclimate/RSL (Littman 2000; Weaver, 2002; Garrison, *et al*, 2008). Pollen results for cores 3 and 5, have confirmed the utility of marine sediment for pollen studies, as have that of others (Heusser, 1983). Litwin and Andrle (1992:92-263) noted a similar pollen composition and abundance at five sites in central and eastern Florida Bay. Their assemblages were dominated by both pine and oak with pine averaging 70% across their samples (*ibid*). A closer inspection of the core 3 data, in terms of actual grains, shows as significant diminishment of oak pollen at 134 cm to 12 grains/spl. compared to that of 30 - 54 grains/spl. Core 5 shows a similar trend - 15 grains/spl. at 171 cm - but a recovery to the expected range 32-56 grains/spl., e.g. 50 grains/spl at 198 cm (Fig. 2).

Another interesting result is the distribution of a third arboreal species - beech (*Fagus*) - in core 3 (Table 3; Fig. 2). This pollen occurs at a range of 2-16 grains/ spl. in four of the eight levels. Likewise, in contrast to the uniformity of pine and oak pollen in both cores, Very little beech appears in core 5 - six levels out of nine but with concentrations of only 1 - 3 grains/spl. Birch (*Betula*) is present in small, but consistent, amounts across both cores (Table 3). Russell, *et al* (2009) state that at LGM, south of 34° N latitude, oaks comprised ~20% of forests. The data for the Gray's Reef cores (Tables 3,4) are comparable. *Liquidambar* (sweet gum), a modern (Holocene) southeastern forest species, is present, in low amounts, in Core 5 (Table 3, fig. 2)(Booth, et al, 1999).

The presence of birch pollen, while in low proportions, like sweet gum, supports Frey's (1953) and Russell, *et al* (2009) contention, at LGM, that Southeastern forests contained a mixture of boreal and austral arboreal species, in "no-analog" plant communities (Overpeck, *et al*, 1985; Delcourt and Delcourt, 1994; Edwards *et al*, 2005). Because of the qualitative nature of the results, Littman's J-Reef pollen data are not shown (Littman, 2000). In those cores, however, boreal and austral taxa were detected. What cannot be determined, in regard to the presence of birch pollen, in the both the Gray's Reef and J-Reef cores, is whether these are tree or shrub birch species. *Betula populifolia* is representative of the former and *B. nigra* the latter category. Neither does birch signal general climate conditions such as "wetter-cooler" or "more arid". The absence of birch pollen in core 3 at the -134 cm level suggests a climate shift that effectively removed birch from the late Quaternary coastal plain such as during a Heinrich Event (3 or 2) when a colder, drier climate would be expected to prevail. Pine and beech are cool-to-cold tolerant species compared to the oak and birch (Preusser et al. 2003:1442). Lachniet et al. (2004), in a characterization of the early Holocene cold event (Veski et al., 2004) at 8200 YBP, observed a sharp increase in both the pollen of *picea* and *betula* (*supra*). Tzedakis et al. (2004), likewise, report tree population changes in the last glacial, e.g., contraction or of observed of temperate species during Heinrich events (HE) 3/2 (ca. 31/24 ka).

O'Kelley's research at Edisto Island, South

Carolina, is similar to that described for Gray's Reef - paleontological and palynological (1976). His work was in the nearshore sediments at Edisto Island where marsh-peat/clay predominate. Radiocarbon ages for the Edisto deposits are within the last 2000 years, as one would expect. In the Edisto data of one core, EB 139A, 55% of the 291 grain-count sample was pine; 12% was oak. This is comparable with our data. Interestingly, while O'Kelley's reports other forest species - sweet gum, maple, hickory and birch he reports no beech (1976:16).

More recently, Groot, *et al* (1995) used palynology, foraminifera analysis and aminostratigraphy to examine sediment cores from continental shelf/slope and coastal deposits in the Delmarva. In that study a 305 m marine core (AMCOR 6021C0 together with AMCOR 6007 and 6008 cores from the nearshore/coastal plain were analyzed Groot, *et al* (1995) examined the AMCOR 6008 core sediments, located 15 km offshore, and determined them to be no older than M.I.S. 5. The pollen therein were parsed into the following categories:

(1)Cold climate taxa:*Picea* and *Abies.*

(2)Temperate and/or warm taxa: *Quercus, Carya, Castanea, Juglans, Liquidambar, Nyssa,* and *Taxodium.*

(3)Herbs and grasses: Chenopodium, Gramineae, Compostitae, Gramineae, Cyperaceae and Ericaeae.

Groot, *et al* (1995 had the advantage of distinguishing six species of oak thereby allowing resolution of older stages than M.I.S. 5 by their presence or absence (ex. *Q. alba*). High percentages of *Pinus* indicated cool-temperate climate. In the lower portions of AMCOR 6007 and 6008 (Pliocene?), higher percentages of *Quercus* were observed in proportion to lower frequencies for *Pinus* (<50%). In the upper (Pleistocene) sections of these cores, *Quercus* increases in relation to *Pinus* (~34-64% versus 3-15%) over the range of M.I.S. 4 to M.I.S.2. As with Grimm, *et al* (1993), these results signaled climatic oscillations. It should be noted that the Delmarva data is reflective of Quaternary conditions in the northern Mid-Atlantic Bight (MAB) and there are salient differences with those from data of the Southeast such as the increased presence of boreal taxa as would be expected of communities near the ice margins.

In eastern North America the climax deciduous forest is dominated at present by maples (O'Kelley reports 4.1%), oaks, hickories and other combinations of trees (such as pines in the southern U.S.) (Stern, 1994:412). Watts, and co-workers, reports a similar vegetational and forest history for the Southeast based on pollen records from White Pond (South Carolina) and Camel Lake (N.W. Florida) (Watts, et al. 1992; Watts, 1980). In these locations, the middle Wisconsin (40-29 ka, M.I.S. 3) was a time of forest abundant pine, oak and diverse mesic tree species such as chestnut (*Castanea*) together with eastern Hemlock (*Tsuga canadensis*) (Watts *et al*, 1992: 1056; Ellison et al. 2005:479-486). The Camel Lake pollen spectra suggest a species-poor pine forest in the Late Wisconsin (after 29 ka or M.I.S. 2).

The pollen stratigraphy for the Gray's Reef cores suggests a temperate coastal plain, parkland biome dominated by pine (*Pinus*) and oak (*Quercus*) in M.I.S. 3. (Figure 3). The persistence of both *Chenopodium* and, to a lesser degree, Ambrosia, throughout cores 3 and 5, suggest a more open type of biome with grassland present (Table 3). In fact the high percentage for *Chenopodium* in the Gray's Reef clay (Table 4) likely correlates with the sharp increase for this taxa in the upper level of core 3 (Table 3, fig. 2). Reconciliation of pollen stratigraphy with the radiometric ages (Table 2)[1] suggests a mid-to-late last glacial (M.I.S. 3) date for the inversion in the oak-pine pollen spectrum, observed in both spectra (Table 3), suggests an expansion of a colder interval - pine increases - at the lower portions of the cores (-134 cm, core 3; -171 cm, core 5). The timing of this excursion, in the pine-oak ratio, suggests a late M.I.S. 3 (H.E. 3/2) date (Watts et al. 1992; Grimm, et al, 2006). (Chappell and Shackleton, 1986). Models for northern hemisphere ice volume show a significant reduction (increase in oak?) in the Farmdale interstade (ca. 25 ka) with increased volume peaks (increased pine?) at the Alton and Woodfordian intervals (ca. 37 and 20 ka. - HE 4/2) Resolution in these models

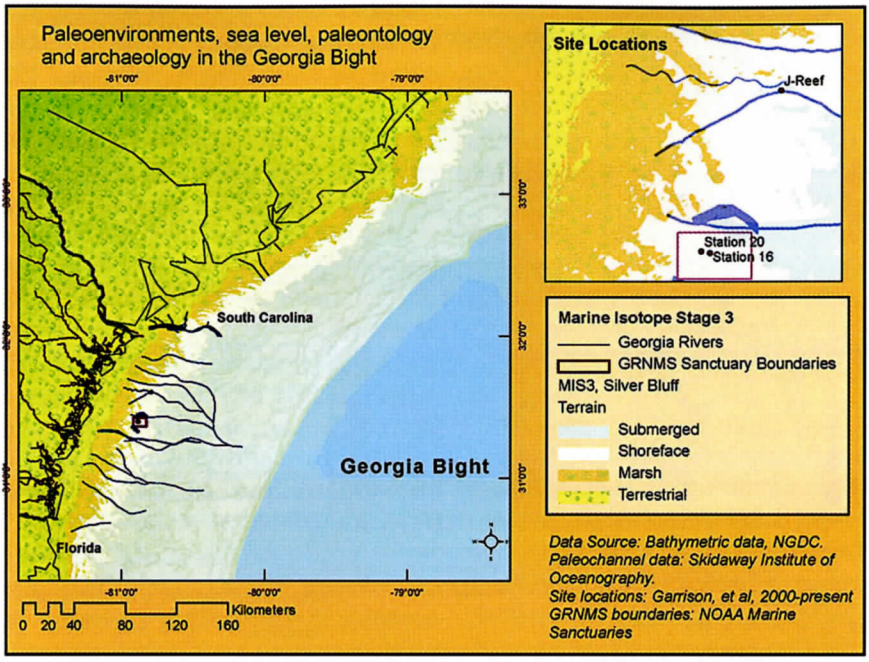

Figure 3a. Sea level and environment reconstruction at 45 ky BP. Biome maps based on this study and others (cf. Russell, *et* al, 2009;Williams, *et al,* 2006).

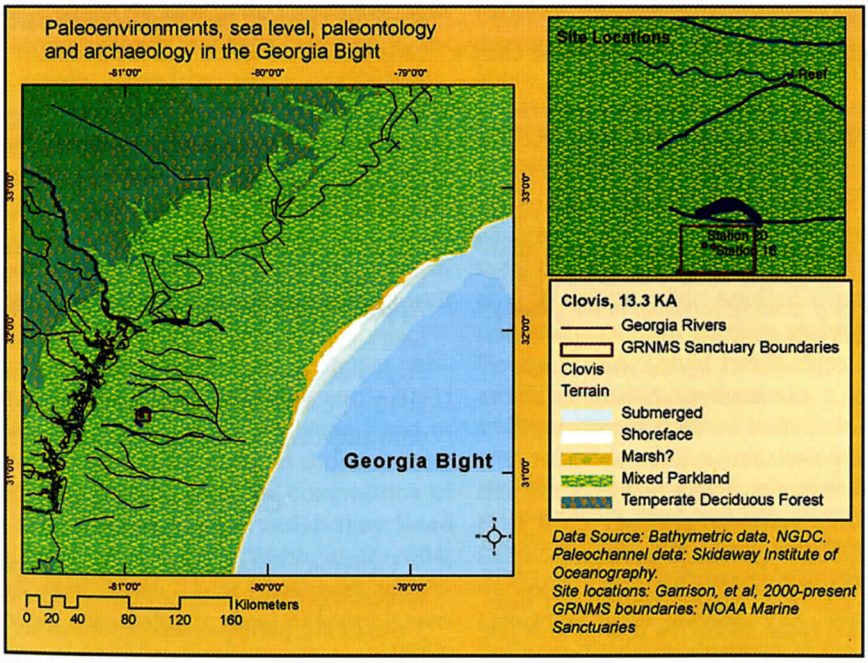

Figure 3b. Sea level and environment reconstruction at 13.3 ky BP. Biome maps based on this study and others (cf. Russell, *et* al, 2009;Williams, *et al,* 2006).

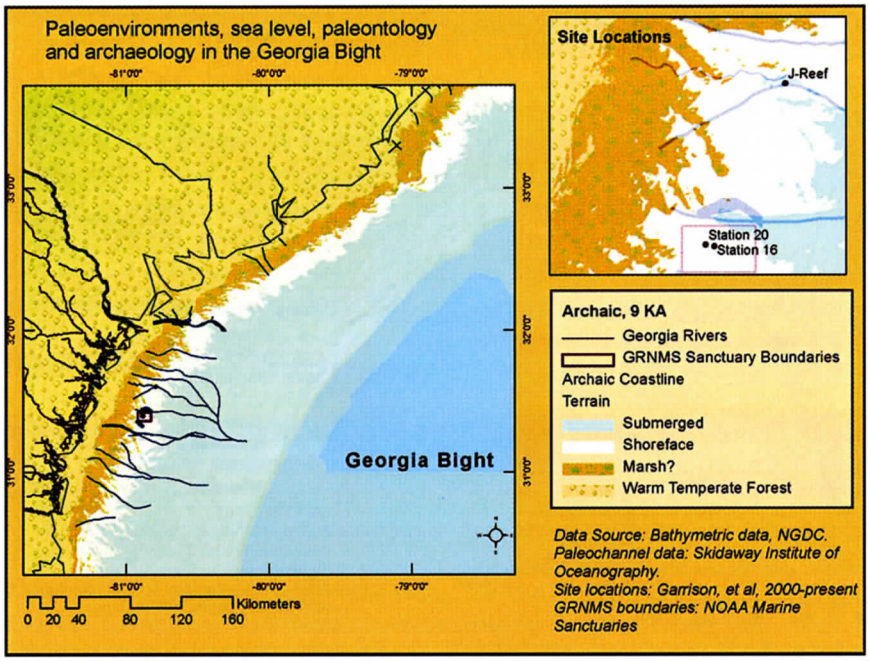

Figure 3c. Sea level and environment reconstruction at 9 ky BP. Biome maps based on this study and others (cf. Russell, *et* al, 2009;Williams, *et al,* 2006).

is generally too coarse to detect millennia - length excursions, in regional climate.

Russell, *et al* (2009:84) conclude the Gray's Reef pollen assemblage documents the presence of "mixed" late Pleistocene-early Holocene floras in Florida and the southern Atlantic seaboard. Around 13,000 k YP, the Warm Mixed Forest Biome (also called the broad-leaved evergreen forest by Williams, et al (2000)) expanded out of the Florida Peninsula into the southeastern lowlands to replace a Mixed Parkland biome while a Temperate Deciduous Forest Biome expanded in the Southern Appalachians and adjacent Piedmont, being well established by the mid-Archaic/mid-Holocene Periods, ca. 9000 y BP (Jardine, et al 2012:31). We illustrate these putative biomes, with attendant sea levels/coastlines in figure 3.

CONCLUSIONS

Extreme climate events can manifest themselves in proxies such as pollen. Between MIS 3 and LGM, perhaps contemporaneous with the HE 4 to HE 2 events, a contraction of temperate arboreal taxa, such as oak, imply a direct climate-ecology coupling. The chronological and

1. By using OSL as a correlative tool, the AMS dates we report are less suspect with regard to well known calibration issues for ages > 30 ka (Richards and Beck, 2001; Van der Plicht, 2002). Because of large fluctuations in atmospheric ^{14}C content in the >30 ka time range, mainly as a result of variation in the geomagnetic field and the North American thermohaline circulation, AMS age estimates can be as much as 7 ka too young (Beck, et al, 2001; Laj, et al, 2002). For AMS dates greater than 42 ka the age offset may be somewhat less, possibly in the 3-4 ka range. Reliable calibration curves for this time range remain elusive (O'Connell and Allen, 2004). Both AMS and OSL dates from Gray's Reef sediments, above 170cm b.s. of 27 kaYBP, suggest this nearshore part of the Satilla Fm is at or near late glacial maximum (LGM- M.I.S. 2) in age (Table 2). Conversely the deeper, ~ 2m b.s., Brown Sand member is at least early glacial, e.g. M.I.S. 3 (Plum Point Inter-Stade?).

sea level data for the Gray's Reef sediment cores indicate a shallow coastal ocean prior to a late MIS 3 coastline. Pine expands, at the expense of oak, in the colder interval detected in the cores 3 and 5. Certainly, HE 3/2, and LGM, can be manifest in the paleoecology. Given the potential for reworking and mixture of the shelf sediments, dating the exact period of the observed shift in arboreal taxa requires more chronological study. We cannot completely rule out LGM as this cold Pleistocene interval within which temperate arboreal species waned and cold tolerant ones waxed. That said, it is important point to note that pollen from marine sediments can be used to map these late Pleistocene climate oscillations in the Southeast. The continental shelf sediments of the Georgia Bight show very little to no lithologic variability (Garrison, *et al*, 2008)). There is, however, significant variability in paleoclimate/paleoecological proxies within these sediments. When coupled with direct dating of these marine sediments, mesoscale – millennial or finer - variation of climate and ecology can be reliably inferred.

MIS 3, which the bulk of the Gray's Reef pollen spectra represents, has been called a non-analog climatic period by paleoclimatologists. Likewise, palynologists and paleoecologists have termed many of the biomes of this period non-analog as well. As pointed out by Russell, *et al* (2009) in their proposal for the Quaternary Southeast as a "thermal enclave", part of the reasons for non-analog communities – plant or animal – are the organisms themselves as well as climate.

The Mixed Parkland biome, no longer present in North America (Williams, et al, 2001) was associated with a Rancholabrean fauna of late Quaternary coastal plain, as different from modern communities as is the composition of plant communities within which they lived (Frey, 1973; Webb, 1977; Webb, *et al*, 2004; Russell, *et al*, 2009). These Quaternary ecosystems were non-analog to those of today (Overpeck *et al* (1985); Graham, *et al,* (1996); Edwards, *et al*, (2005); Williams, *et al*, (2004); and Russell, *et al*, (2009)). As we suggest, part of this difference is at the ecosystem level where Quaternary fauna grazed and browsed a coastal plain biome that was more parkland than forest due to climate, but, also, in large part, to the fauna themselves. As Williams, et al (2001) opin, plant associations with no modern analog, such as the Mixed Parkland, grew in environments outside the range of modern climate space. The Quaternary coastal plain that included Gray's Reef, particularly in MIS 3, was just such a climate space.

ACKNOWLEDGMENTS

The authors wish to thank the National Oceanic and Atmospheric Administration (NOAA), Gray's Reef National Marine Sanctuary, for support of this research since 1995. Reed Bohne, was instrumental in initiating and providing financial as well as in-kind support. Dr. George Sedberry, Sanctuary Manager has continued this support. The Sanctuary staff has given generously of their time and expertise, in particular, Greg McFall, Deputy Sanctuary Manager and Research Coordinator. Likewise the officers and crew of the former NOAA Research Ship FERREL provided invaluable vessel support during geophysical and geological coring operations in 1995, 1996, 1999 and 2000.

Dr. Paul Gayes, Coastal Carolina University and Dr. John Anderson, Rice University, provided critical vibracoring equipment to the project and are thanked for their collegiality and generosity.The University of Georgia's Department of Geology; the Department of Geography; The Center for Applied Isotope Studies provided analytical services and support. Drs. George Brook, David Leigh, Alex Cherkinsky and Scott Noakes are thanked.

The authors benefited from their discussions with numerous colleagues during the preparation of this paper. These colleagues include Dr. Fred Rich, Georgia Southern University; Dr. Clark Alexander, Skidaway Institute of Oceanography; Dr. John Wehmiller, University of Delaware; Brian Thomas, TRC, Inc., and Mike Sullivan, Skidaway Institute of Oceanography. Other colleagues whom we have missed in these acknowledgements are thanked for all their advice and assistance. Any errors or mis-

interpretations are entirely those of the authors.

REFERENCES

Antoine, J.W. and V.J. Henry, 1965. Seismic refraction study of shallow part of continental shelf off Georgia coast. *Am. Assoc. Petrol. Geol. Bull.*, 49:601 - 609.

Beck, J.W., D.A. Richards, R.L. Edwards, B.W. Silverman, P.L. Smart, D.J. Donahue, S. Herrera-Osterheld, G.S. Burr, L. Calysas, A.J.T. Jull, D. Biddulph. 2001. Extremely large variations of atmospheric ^{14}C during the last glacial period. *Science*, 292: 2453 – 2458.

Booth, R.K., F.J. Rich and G. Bishop. 1999. Palynology and depositional history of late Pleistocene and Holocene coastal sediments from St. Catherines Island, Georgia, U.S.A. *Palynology*, 23:67-86.

Buffler, R.T., J.S. Watkins, and W.P. Dillon, 1978. Geology of the Southeastern Georgia Embayment, U.S. Atlantic Continental Margin, based on Multichannel Seismic Reflection Profiles. *AAPG Memoir*, 29:11-25

Chappell, N. and J.F. Shackleton. 1986. Oxygen isotopes and sea level. *Nature* 324:137-140

Delcourt, H.R. and P.A. Delcourt. 1994. Postglacial rise and decline of *Ostrya virginiana* (Mill.) K. Koch and *Carpinus caroliniana* Walt. in eastern North America: predictable responses of forest species to cyclic changes in seasonality of climates. *Journal of Biogeography*, 21(2):137-150.

Duane, D.B., M.E. Field, E.P. Meisburger, D.J.P. Swift, and S.J. Williams. 1972. Linear shoals on the Atlantic continental shelf, Florida to Long Island. In D.J.P. Swift, D.B. Duane and O.H. Pilkey (editors), *Shelf Sediment Transport – Process and Patterns.* Dowden, Hutchinson and Ross, Inc. Stroudsburg, PA.Pp. 447-498.

Duller, GAT, L. Botter-Jensen, and V. Mejdahl. 1999. An automated iterative procedure for determining palaeodoses using the SARA method. *Quat. Sci. Rev.* 18(2): 293-301.

Edwards, M.E., L.B. Brubaker, A.V. Lozhkin and P.M. Anderson. 2005. Structurally novel biomes: a response to past warming in Beringia. *Ecology*, 86:1696-1703.

Ellison, A. M., M. S. Bank, B. D. Clinton, E. A. Colburn, K. Elliott, C. R. Ford, D. R. Foster, B. D. Kloeppel, J. D. Knoepp, G.M. Lovett, J. Mohan, D. A. Orwig, N.L. Rodenhouse, W.V. Sobczak, K.A. Stinson, J.K. Stone, C.M. Swan, J. Thompson, B. Von Holle, and J.R. Webster. 2005. Loss of foundation species: consequences for the structure and dynamics of forested ecosystems. *Frontiers in Ecology and the Environment* **3**: 479–486.

Foyle, A.M., V.J. Henry and C.R. Alexander. 2004. Georgia-South Carolina Coastal Erosion Study: Phase 2 Southern Study Region State of Knowledge Report & Semi-Annotated Bibliography. Skidaway Institute of Oceanography. Savannah, GA. 251 pages.

Foyle, A.M. and V.J. Henry. 2004, submitted. Groundwater study reveals new details on the Cenozoic stratigraphic framework and Quaternary paleodrainage networks at the apex of the Georgia Bight. *Southeastern Geology.*

Frey, D.G. 1953. Regional aspects of the late-glacial and post glacial pollen succession of southeastern North Carolina. *Ecological Monographs*, 23:289-313.

Frey, R.W. (Ed.), 1973. *The Neogene of the Georgia Coast.* Department of Geology, University of Georgia, Athens.

Garrison, E.G., G. McFall and S. E. Noakes. 2008. Shallow Marine Margin Sediments, Modern Marine Erosion and the Fate of Sequence Boundaries – Georgia Bight (USA) *Southeastern Geology*, 45:127-142.

Gayes, P.T., D.B. Scott, E.S. Collins, and D.G. Nelson. 1992. Quaternary coasts of the United States: marine and estuarine systems. *SEPM publication No. 48.*

Gonzalez, C. and L.M. Dupont. 2009. Coastal vegetation evidence for sea level changes associated with Heinrich Events. *PAGES NewS*, 17(2): 70-72.

Graham R.W., E.L. Lundelius Jr., M.A. Graham, E.K. Schroeder, R.S. Toomey III, E. Anderson, A.D. Barnosky, J.A. Burns, C.S. Churcher, D.K. Grayson, R.D. Guthrie, C.R. Harington, G.T. Jefferson, L.D. Martin, H.G. McDonald, R.E Morlan, H.A. Semken Jr., S.D.Webb, L.Werdelin, and M.C. Wilson.1996. Spatial response of mammals to late Quaternary environmental fluctuations. Science, 272:1601-6.

Grimm, E.C., G.L. Jacobson Jr., W.A. Watts, B.C.S. Hansen and K.A. Maasch 1993. A 50,000- year record of climate oscillations from Florida and its temporal correlation with the Henirich events. *Science*. 261:198-200.

Grimm, E.C., W.A. Watts, G.L. Jacobson Jr., B.C.S. Hansen, H.R. Almquist, and A.C Dieffenbacher-Krall. 2006. Evidence for warm wet Heinrich events in Florida. *Quaternary Science Reviews*, 25:2197-2211.

Groot, J.J., R.N. Benson and J.F. Wehmiller.1995. Palynological, foraminiferal and aminostratigraphic studies of Quaternary sediments from the U.S. middle Atlantic upper continental slope, continental shelf and coastal plain. *Quaternary Science Reviews*, 14:17-49.

Harding, J.L., and V.J. Henry, 1994. Geological History of Gray's Reef National Marine Sanctuary. Report to the National Oceanic and Atmospheric Administration. 10 Ocean ScienceCircle, Savannah, GA 30411.

Hemmings, S.R. 2004. Heinrich events: massive late Pleistocene detritus layers in the North Atlantic and their global climate imprint. *Reviews of Geophysics*, 42, RG1005.

Henry, V.J. Jr., C.J. McCreery, F.D. Foley and D.R. Kendall. 1981. Ocean bottom survey of the Georgia Bight. In: P. Popenoe (editor), Environmental Geologic Studies on theSoutheastern Atlantic Outer Continental Shelf, 1977-1978, *U.S. Geological Survey Open-FileReport 81-582-A*: 6-1 - 6-85, U.S. Geological Survey, Woods Hole, Massachusetts.

Henry, V.J. and F.M. Idris. 1992. Offshore minerals assessment studies on the Georgia continental shelf – Phase 2: Seismic stratigraphy of the TACTS area and evaluation of selected sites for economic hard minerals potential. *Georgia Department of Natural Resources Project Report 18*, Atlanta, Georgia, 143 p.

Heusser, L.E. 1983. Pollen Distribution in the Bottom Sed-

iments of the Western North Atlantic Ocean, *Marine Micropaleontology*, 8:77 -88.

L.E. Heusser and C.E. 1984. Stock Preparation Techniques for Concentrating Pollen from Marine Sediments and Other Sediments with Low Pollen Density.*Palynology*, 8:225-227.

Howard, J.D. and H.D. Reineck, 1972. Georgia coastal region, Sapelo Island, U.S.A.: Sedimentology and biology. IV. Physical and biogenic structures of the nearshore shelf. *Senkenberg. Marit.* 4:81-123.

Howard, J.D., R.W. Frey, and H.E. Reineck, 1973. Holocene sediments in the Georgia coastal area. In Frey, R.W. (Ed) 1973. *The Neogene of the Georgia Coast.* Department of Geology, University of Georgia, Athens.

Huddleston, P.F., 1988. A revision of the lithostratigraphic units of the coastal plain of Georgia - Miocene through Holocene. *Georgia Geological Survey Bulletin,* 104.

Idris, F.M. and V.J. Jr. Henry. 1995. Shallow Cenozoic stratigraphy and structure: South

Carolina lower coastal plain and continental shelf. *GSA Bulletin*, 107: 762-778.

Indurante, S.J., L.R. Follmer, R.D. Hammer, and P.G. Koenig, 1980. Particle size analysis by a modified pipette procedure. *Soil Science Society of American Journal,* 54: 560-563.

Jardine, P.E., G.J. Harrington and T.A. Stidham. 2012. Regional-scale heterogeneity in the late Paleocene paratropical forest of the U.S. Gulf Coast. *Paleobiology 38(1): 15-39.*

Lachniet, M.S., Y. Asmerom, S.J. Burns, W. P. Patterson, V. J. Polyak and G. O. Seltzer 2004. Tropical response to the 8200 yr B.P. cold event? Speleothem isotopes indicate a weakened early Holocene monsoon in Costa Rica.*Geology,*32(11):957-960.

Laj, C., C. Kiessel, A. Mazaud, E. Michel, R. Muschler and J. Beer. 2002. Geomagnetic field intensity, North American Deep Water circulation and atmospheric delta C-14 during the last 50 kyr. *Earth and Planetary Science Letters*, 200:177-190.

Littman, S., (2000). Pleistocene/Holocene sea level change in the Georgia Bight: a paleonenvironmental reconstruction of Gray's Reef National marine Sanctuary and J. Reef. Unpublished Master's thesis, University of Georgia, Athens.

Litwin, R.J. and V.A.S. Andrle. 1992. Modern palynomorph and weather census data from the U.S. Atlantic coast (Continental Margin Program samples and selected NOAA weather stations). *USGS Open File Report 92-263*, 31 pages.

Litwin, R.J., M.J. Pavich, and H.W. Markewich. 2010. HYBLA CORES 7 & 8: An 80,000-year late Pleistocene climate record from the mid-Atlantic coastal plain of North America. Abstract,0032. Northeastern Section (45th Annual) and Southeastern Section (59th Annual) Joint Meeting of the Geological Society of America. Baltimore, MD, March 13-16.

Markewich H.W., J.R. Litwin, M.J. Pavich, and G. A. Brook. 2009. Late Pleistocene eolian features in southeastern Maryland and Chesapeake Bay region indicate strong WNW–NW winds accompanied growth of the Laurentide Ice Sheet. *Quaternary Research*, 71:409-425.

Milliman, J.D., O.H. Pilkey, and D.A. Ross. (1972). Sediments of the continental margin off the eastern United States. Geology Society of America Bulletin, 83: 1315-1334.

Murray A.S. and A.G. Wintle. 2000. Dating quartz using an improved single-aliquot regenerative dose (SAR) protocol. *Radiation Measurements*, 32:57-73.

O'Connell, J.F., and J. Allen, 2004, Dating the colonization of Sahul (Pleistocene Australia-New Guinea): a review of recent research: *Journal of Archaeological Science*, 31:835-853

O'Kelley, R.V., 1976. Late Quaternary Vertebrate Fossils and Pollen from Edisto Island, South Carolina. Unpublished Masters thesis. University of Georgia, Athens.

Overpeck, J.T. Webb, T. III, and I.C. Prentice 1985.Quantitative interpretation of fossil pollen spectra: Dissimilarity coefficients and the method of modern analogs. *Quaternary Research*, 23(1): 87-108.

Pieñkowski, G. and M. Waksmundzka. 2009. Palynofacies in Lower Jurassic epicontinental deposits of Poland: tool to interpret sedimentary environments. *Episodes*, 32(1):22-32.

Pilkey, O.H., B.W. Blackwelder, H.I. Knebel and M.W. Myers, 1981. The Georgia Embayment continental shelf: stratigraphy of a submergence. *Geological Society of American Bulletin,* 92:52-63.

Pilkey, O.H., and D. Frankenberg, 1964. The relict-recent sediment boundary on the Georgia Continental Shelf. *Bulletin of the Georgia Academy of Science*, 22:37-40.

Preusser, F., M.A. Geyh and C. Schlücter. 2003. Timing of Late Pleistocene change in lowland Switzerland. *Quaternary Science Reviews*, 22: 1435-1445.

Richards, D.A. and J.W. Beck, 2001. Dramatic shifts in atmospheric radiocarbon during the Last Glacial Period. *Antiquity*, 73: 482-485.

Richter, H. G. 1985. Wood and bark anatomy of Lauraceae II. Licaria Aublet. *IAWA Bulletin*, 6(3):187-199.

Russell, D.A., F.J. Rich, V. Schneider and J. Lynch-Stiegliz. 2009. A warm thermal enclave in the late Pleistocene of the south-eastern United States. *Biological Reviews*, 84:173-202.

Sexton, W.J., M.O. Hayes and D.J. Colquhoun, 1992. *Evolution of Quaternary shoal complexes of the south central South Carolina coast. Quaternary Coasts of the United States: marine and Lacustrine Systems.* SEPM Special Publication No. 48. SEPM, Tulsa, OK.

Shane, L.C.K. 1992. Palynological Procedure. Unpublished training documents for University of Minnesota Limnological Research Center. 19 pages.

Siddall, M., E.J. Rohling, W.G. Thompson and C. Waelbroeck. 2008. Marine isotope stage 3 sea level fluctuations: data synthesis and new outlook. Reviews of Geophysics, 46:1-29

Stern, R.V., 1994. Introductory Plant Biology. William C.

Brown Publishers. Dubuque, IA.

Stewart, J.R. 2005. The ecology and adaptation of Neanderthals during the non-analogue environment of Oxygen Isotope Stage 3. *Quaternary International*, 137:35-46.

Swift, D.J.P., J.W. Kofoed, F.P. Saulberg and P. Sears. 1972. Holocene evolution of the shelf surface, central and south Atlantic shelf of North America, in Swift, D.J.P., D.B. Duane, and O.H. Pilkey, eds. *Shelf Sediment, Transport, Process and Pattern*. Dowden, Hutchison and Ross, Stroudsburg, PA. Pp. 499-574

Swift, D.J.P. and A.W. Niedoroda. 1985. Fluid and sediment dynamics on continental shelves, in R.W. Tillman, D.J.P. Swift and R.G. Walker, eds. *Shelf Sands and Sandstone Reservoirs: Society* of *Economic Paleontologists and Mineralogists Short Course No. 13.* Pp. 47-133.

Tzedakis, P.C., M.R. Frogley, I.T. Lawson, R.C. Preece, I. Cacho and L. de Abreu. 2004.Ecological thresholds and patterns of millennial-scale climate variability: The response of vegetation in Greece during the last glacial period. *Geology,* 32:109-112.

Van der Plicht, J. 2002. Calibration of the C-14 time scale: towards a complete dating range, Geologie en Mijnbouw-Netherlands. *Journal of Geosciences*, 81:85-96.

B. van Geel, V.G. Dirksen, G.I. Zaitseva, N.A. Bokovenko, N.D. Burova, M. Kukova, H. Parzinger, A. Nagler, K.V. Chugunov, V.A.Dergachev, S.S. Vasiliev and J. van der Plicht.2006. Reply to S. Riehl and K. Pustovoytov. *Journal of Archaeological Science*,33:143–144)

Veski, S., H. Seppa, and A.E.K. Ojala. 2004. Cold event at 8200 B.P. recorded in annually laminated lake sediments in eastern Europe. *Geology*, 32: 681-684.

Watts, W.A. 1980. Late-Quaternary vegetation at White Pond on the inner coastal-plain of South Carolina. *Quaternary Research*, 13: 187-199.

Watts, W.A., B.C.S. Hansen, and E.C. Grimm, 1992. Camel Lake: A 40,000-yr record of vegetational and forest history from northwest Florida. *Ecology.* 73(3): 1056-1066.

Weaver, W., 2002. Paleoecology and Prehistory: Fossil Pollen at Gray's Reef National Marine Sanctuary. Masters thesis. University of Georgia, Athens.

Webb, S. D. 1977. A History of Savanna Vertebrates in the New World. Part I: North America *Annual Review of Ecology and Systematics* 8: 355-380.

Webb, S.D., R.W. Graham., A.D. Barnosky, C.J. Bell, R. Franz, E.A. Hadly, E.L. Lundelius, Jr., H. G. McDonald, R.A. Martin, H.A. Semken, Jr. and D.W. Steadman. 2004. Vertebrate Paleontology. In Developments in Quaternary Science, 1, Series Editor: J. Rose., *The Quaternary Period in the United States*. Eds. A.R. Gillepsie, S.C. Porter and B.F. Atwater. Elsevier. Amsterdam.

Wehmiller, J., E.R. Thieler, D. Miller, V. Pellerito, V. Bakeman Keeney, S.R. Riggs, S. Culver, D. Mallinson, K.M. Farrell, L.L. York, J. Pierson ad P.R. Parham. 2010. Aminostratigraphy of surface and subsurface sediments, North Carolina coastal plain. *Quaternary Geochronology*, 5:459-492.

Williams, J.W., T. Webb III, P.H. Richard and P.Newby. 2000. Late-Quaternary biomes of Canada and the eastern North America. *Journal of Biogeography*, 27:585-607.

Williams, J.W., B.N. Shuman and T. Webb III. 2001. Dissimilarity analyses of late-Quaternary vegetation and climate in eastern North America. *Ecology*, 82:3346-3362.

Williams, J.W., Shuman, B.N., Webb III, B*artlein, P.J.* and P.L.L*educ.* 2004. Late Quaternary vegetation in North America: scaling of taxa to biomes. *Ecological Monographs*, 74:309-324.

Williams, J.W. and S.T. Jackson. 2007. Novel climates, no-analog communities, and ecological surprises. *Frontiers in Ecology and Environment,* 5(9):475-482.

Williams, K. M., J. T. Andrews, N. J. Weiner and P. J. Mudie. 1995. Late Quaternary Paleoceanography of the Mid- to Outer Continental Shelf, East Greenland, *Arctic and Alpine Research,* 27(4): 352-363.

Woolsey, J.R., 1977. Neogene stratigraphy of the Georgia coast and inner continental shelf. Unpublished. University of Georgia, Athens.

Woolsey, J.R. and V. J. Henry, 1974. Shallow, high resolution investigations of the Georgia coast and inner continental shelf. In *Symposium of the Petroleum Geology of the Georgia Coastal Plain: Georgia Geological Survey Bulletin,* 87: 167 -187.

SOUTHEASTERN GEOLOGY
V. 48, No. 4, February 2012, p. 185-206

MAJOR AND TRACE ELEMENT GEOCHEMISTRY OF THE SOAPSTONE RIDGE COMPLEX IN GEORGIA, SOUTHERN APPALACHIANS

JEFF B. CHAUMBA*

Department of Geology, University of Georgia
Athens, GA 30602
**Department of Geology and Geography*
Auburn University
Auburn, Alabama 36849
Email: chaumba@auburn.edu

ABSTRACT

A study of bulk-rock compositions and CIPW norms of the Soapstone Ridge complex (SSR), supplemented by the extensive data from Higgins and others (1988), has been conducted on rocks in order to constrain its origin. Major and trace element concentrations of compatible elements from the SSR such as MgO and Ni are much higher than those of melts, consistent with a cumulate origin for most SSR rocks.

Normative calculations indicate that approximately half of the bulk-rock major element data in Higgins and others (1988) have normative corundum contents ranging from 1 to 7.3 wt.%. Silica contents from all samples of the SSR range from 45 to 57 wt.% SiO_2 indicating that the rocks are dominantly basic to intermediate. Based of CIPW norm plots, SSR rock types are mostly metapyroxenites and metagabbros with very few metaperidotites. Rocks from the SSR have high normative pyroxene contents, generally low normative plagioclase contents, and low to moderate normative olivine contents. Bulk-rock compositions from the SSR are akin to those formed in some island arc settings, such as the Solomon Islands, lending support to an origin as an intra-oceanic arc crust.

INTRODUCTION

The Soapstone Ridge complex (SSR) is the largest mafic/ultramafic body in the southern Appalachians (Higgins and others, 1980). Recent mapping shows that the SSR is a sheet-like body that covers approximately 40 km^2 and has a maximum thickness of 200 m (Higgins and others, 1980; Higgins and Atkins, 1981; Higgins and Crawford, 2007).

Hatcher and others (2007) recently published a new tectonic map of the central and southern Appalachians based on recent mapping and geochronologic data (Figure 1). Rocks of the SSR are metamorphosed mafic and ultramafic rocks that outcrop in the Tugaloo terrane of the southern Appalachian orogen (Figure 1). Rock types of the SSR include metapyroxenites, metatroctolites, metagabbros, and meta-anorthosites (Higgins and others, 1988). According to Higgins and others (1980), 90% of the rocks comprising the SSR are mafic, with the remainder being ultramafic. Protoliths of SSR rocks were first interpreted as altered gabbros and gabbros (Higgins, 1966; Pickering and others, 1972), and then, later, as various rock types interpreted to be relict ocean floor and mantle rocks, i.e., part of an ophiolite (Higgins and others, 1980, 1984, 1988; Higgins and Atkins, 1981). The purpose of this study was to describe the rock types and bulk-rock geochemistry of the SSR, and to place some constrains on the origin and tectonic setting of the SSR based on bulk-rock geochemical data.

SSR bulk-rock geochemical data are presented in Higgins and others (1988), but neither sample locations nor sample descriptions are offered. With the exception of rare earth element plots, no bulk-rock geochemical plots are presented by Higgins and others (1988). Primary geochemical data used in this investigation are from Higgins and others (1988) and they are

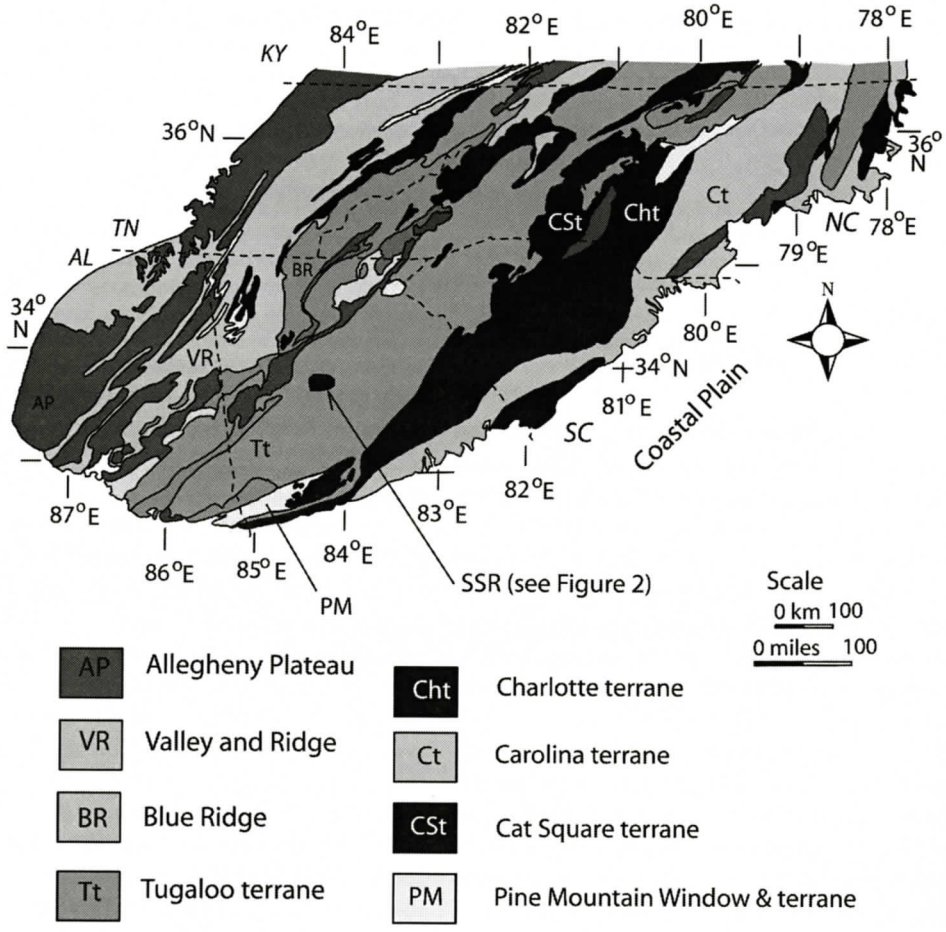

Figure 1. Simplified tectonic map of the southern Appalachians showing the location of the Soapstone Ridge complex (modified from Hatcher and others, 2007).

expanded in scope by new data from eight samples collected during this study.

PREVIOUS WORK ON SOAPSTONE RIDGE COMPLEX

The name "Soapstone Ridge" was used by Hopkins (1914) to describe the largest outcrops of soapstone deposits located in Lumpkin County in northeast Georgia. According to Hopkins (1914), rocks of the SSR in DeKalb County, the subject of the present investigation, were derived from pyroxenites and are now composed of chlorite, talc, amphibole, and magnetite. Hopkins (1914) described the SSR as a soapstone and pyroxenite deposit on a map of the area. The first detailed study of SSR was by Higgins and others (1980) who interpreted the rocks as a dismembered ophiolite tectonically emplaced along a 150-200 m-thick folded imbricate thrust sheet termed the Soapstone Ridge thrust sheet (Figure 2). The altered nature of the SSR rocks was noted by these workers who concluded that hydrothermal alteration and metamorphism affected the mineralogy and the bulk-rock major, trace, and rare-earth element chemistry.

SSR rocks overlie rocks of the Ropes Creek and Paulding thrust sheets which were both metamorphosed under amphibolite facies con-

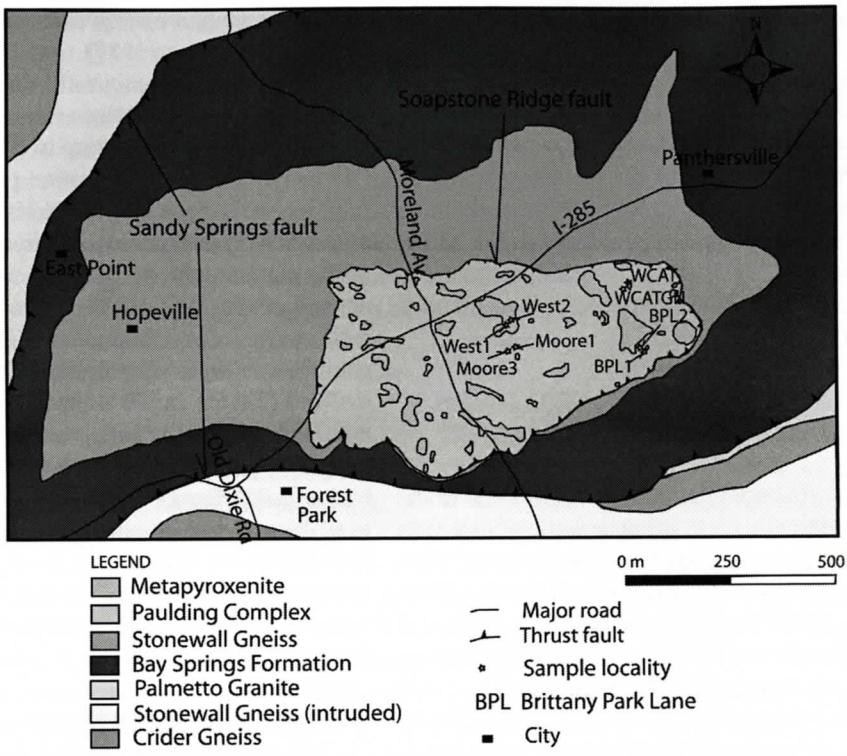

Figure 2. Geologic map of the Soapstone Ridge complex and adjacent areas (after Higgins and Crawford, 2007) showing location of samples in this study.

ditions. The Soapstone Ridge fault truncates folds, quartz veins, and pegmatites of the underlying rocks (Higgins and others, 1984, 1988; Higgins and Crawford, 2007).

Higgins and others (1980) interpreted the southern Appalachians orogen to be composed of three stacks of folded thrust sheets: the lowermost is the Rome-Kingstone thrust stack, which is overlain by the Georgiabama thrust stack, which in turn is overlain by the Little River thrust stack. The Soapstone Ridge thrust sheet is the uppermost of the Georgiabama thrust stacks. The Soapstone Ridge thrust sheet traveled first in a westward direction and the furthest distance from its position in the eastern part of the ancient Iapetus Ocean, compared to all the thrust sheets which comprise the Georgiabama thrust stack (Higgins and others, 1984, 1988). Higgins and others (1988) interpret thrusting to be of Middle Ordovician (Taconic orogeny) to Carboniferous (Alleghanian orogeny) times. Metamorphism of SSR rocks is described as synthrusting by Higgins and others (1988).

BASIC AND ULTRABASIC ROCKS OF THE SOUTHERN APPALACHIANS

Metamorphosed mafic and ultramafic rocks occur as small and isolated bodies throughout the southern Appalachian orogen (Misra and Keller, 1978; Misra and McSween, 1984). Historically, two belts of metamorphosed mafic and ultramafic rocks are depicted in the southern Appalachians (Pratt and Lewis, 1905; Hess, 1955; Larrabee, 1966). One belt occurs to the west of a central axis of intense deformation in the Blue Ridge, whereas the other occurs to the east in the Inner Piedmont and the Carolina zones of the Piedmont (Hibbard and others, 2002; Bream and others, 2004; Hatcher and others, 2005). The belt of metamorphosed mafic/ultramafic bodies which occurs to the west of

the central axis of intense deformation in the Blue Ridge lies in the western Blue Ridge (Misra and Keller, 1978).

SSR is part of the eastern belt of metamorphosed mafic/ultramafic bodies which occurs in the Piedmont. Most of the metamorphosed ultramafic bodies in both the Blue Ridge and Piedmont are Alpine-type with lens-like bodies enclosed in the regional foliation without any evidence of intrusion such as chilled margins (Misra and Keller, 1978).

BASIC AND ULTRABASIC ROCKS OF THE PIEDMONT

The Piedmont belt of metamorphosed mafic and ultramafic rocks is not as well defined as its Blue Ridge counterpart, but can be traced from Alabama to Virginia (Pratt and Lewis, 1905; Hess, 1955; Larrabee, 1966). The Piedmont metamorphosed mafic and ultramafic rocks are composed mostly of chlorite amphibole schists. Talc is locally important and olivine and pyroxene occur in some rocks. The larger occurrences of metamorphosed mafic and ultramafic bodies in the southern Appalachians Piedmont Province are reviewed below.

SOUTH CAROLINA METAMORPHOSED MAFIC AND ULTRAMAFIC BODIES

The Hammett Grove Meta-igneous Suite (HGMS), located in northwestern South Carolina, was examined by Mittwede and others (1987), Mittwede (1989), and Mittwede and Sharp (1990). The HGMS is comprised of metapyroxenites, metagabbros and metabasalts and an altered ultrabasic component composed of soapstone and serpentinite which Mittwede (1989) refers to as an ultramafite. Mittwede (1989) interpreted the HGMS to be a disrupted ophiolite sequence composed of ultramafic and mafic rocks that formed as fore-arc basement to the Carolina superterrane.

The Clemson, Seneca, and Walhalla ultramafic bodies occur in the Tugaloo terrane of western South Carolina (Warner and others, 1986, 1989). The rocks are composed mostly of chlorite, calcic amphibole, olivine, and serpentine. Warner and others (1989) note that moderate amounts of olivine occur either as elongated crystals up to 1.5 cm long or as a fine-grained aggregate forming lenses up to 5cm in length. Olivine lenses show elongation parallel to the foliation in the enclosing rocks, and Warner and others (1989) interpreted the olivine to be part of the metamorphic mineral assemblage. Warner and others (1986, 1989) proposed that these rocks were derived from aluminous peridotitic cumulate sections of ophiolites. Chondrite normalized (Taylor and McLeman, 1985) lanthanum/samarium $(La/Sm)_N$ values range from low values of 0.616 for the Walhalla body to a high of 2.256 for the Seneca body, using the data of Warner and others (1989). Overall, REE abundances are higher than those from cumulate gabbros from ophiolites and the REE patterns are flatter than ophiolite cumulate gabbros.

VIRGINIA METAMORPHOSED MAFIC/ULTRAMAFIC BODIES

Owens and Uschner (2001) described metamorphosed ultrabasic rocks (chlorite amphibole schists, carbonate chlorite-talc schists, chlorite talc schists and chlorite schists) exposed in the central Virginia Piedmont. The rocks display a wide range in bulk compositions. Mg# (atomic 100 x Mg/(Mg + Fe)) range from approximately 73 to 92, and anhydrous SiO_2 contents range from 31 to 63 wt.%. Normative mineralogy includes plagioclase (from 1 to 42%) along with pyroxene (from 9 to 78%) and olivine (from 0 to 53%). Some samples contain appreciable amounts normative corundum (18 and 20%). Despite the abundance of normative plagioclase, the rocks do not show evidence (e.g. elevated Sr or Eu contents) of plagioclase in the protoliths. $(La/Sm)_N$ values for rocks from the central Virginia Piedmont range from low values of 0.612 in a chlorite amphibole schists to a high value of 4.44 in a carbonate-chlorite talc schist from the data of Owens and Uschner (2001).

Rare earth element plots presented by Owens and Uschner (2001) are characterized by cross-

ing patterns that show a wide variation in their concentrations. These are interpreted to be either a result of original REE heterogeneities or of element mobility (Owens and Uschner, 2001). Metasomatic alteration of some ultramafic rocks produced the protoliths for the talc-chlorite schist and carbonate-chlorite-talc schist (Owens and Uschner, 2001). Talc-chlorite schists are interpreted to be metasomatized, but chlorite-amphibole schists are interpreted to be metamorphosed amphibole-bearing peridotites, probably emplaced in a mélange complex (Owens and Uschner, 2001).

NORTH CAROLINA PIEDMONT PROVINCE METAMORPHOSED MAFIC/ULTRAMAFIC BODIES

The Halifax County complex occurs in the eastern part of the state and is composed, from west to east, of metaperidotites, metadunites, metapyroxenites, metagabbros, and meta-anorthosites, quartz diorite, plagiogranite, and metabasalts, resting on a mylonite zone to the west (Kite and Stoddard, 1984). Atlantic Coastal Plain sediments cover the complex to the east. The complex was interpreted by Kite and Stoddard (1984) to have basaltic rocks that are more akin to both island arc basalts and to ocean floor basalts. The Halifax County complex as a whole was interpreted to represent the underpinnings of the Eastern slate belt (Carolina superterrane) volcanic arc (Kite and Stoddard, 1984).

METAMORPHOSED MAFIC AND ULTRAMAFIC ROCKS IN GEORGIA

The Berner Mafic Complex in central Georgia was examined by Hooper and Hatcher (1989). The complex is composed of amphibolites and metagabbros. Hooper and Hatcher (1989) interpreted the basic and ultrabasic rocks of the Berner Mafic Complex to be co-magmatic based on compatible trends on variation diagrams and spatial relationships. The Berner Mafic Complex is described as part of an evolved arc complex, but subsequent deformation and metamorphism makes determination of protoliths of the meta-ultramafic rocks difficult (Hooper and Hatcher, 1989).

Allard and Whitney (1994, 1995) identified over eighty occurrences of basic and ultrabasic rocks in northeast Georgia, which they termed the Russell Lake Allochthon (RLA). Based on horizontal shear zones at the base of these bodies, low-metamorphic grade, and lack of penetrative deformation, Allard and Whitney interpreted these bodies to be part of a large allochthonous sheet - the RLA. Recent studies (Chaumba and Roden, 2007) show that amphiboles and plagioclases in RLA rocks are zoned. The amphibole cores are composed of magnesiohornblende, whereas the rims are composed of actinolite. Plagioclase has anorthite-rich cores and anorthite-poor rims. This sequence of mineral replacement is consistent with early amphibolite and later greenschist facies metamorphic conditions (Chaumba and Roden, 2007).

Higgins and Crawford (2007) recognize two rock units in the SSR. Rocks of the Paulding Volcanic/Plutonic Complex are the most common. This unit is heterogeneous consisting of epidote-chlorite amphibolite, biotite gneisses and schists, and felsic plutonic rocks (Higgins and Crawford, 2007). A second map unit, called metapyroxenites, is composed of rocks with large (4-6 cm) euhedral pseudomorphs of pyroxene now replaced by chlorite, talc, and tremolite/actinolite. Metapyroxenites crop out as rounded boulders and are covered by a thin red soil with sparse vegetation. SSR rocks are correlative with rocks the RLA (Higgins and Crawford, 2007).

In summary, the metamorphosed mafic and ultramafic bodies in the Piedmont region of the southern Appalachians are dominantly composed of metagabbros and metapyroxenites, with relatively few metaperidotites (i.e., metalherzolites, metaharzburgites, metadunites, and metawehrlites). These rocks are thought to have been formed under a variety of settings, ranging from ocean floor rock settings, through island arc settings, and as mélanges. Thus, metamorphosed mafic and ultramafic rocks probably originated under diverse settings, although some show some similarities. For example,

Figure 3. Photograph of a megacrystic meta-orthopyroxenite showing relict cumulate texture defined by very coarse-grained crystals of orthopyroxene and amphibole in a matrix of mostly amphibole.

rocks of the SSR are thus broadly comparable to other metamorphosed mafic and ultramafic rock types from the Tugaloo terrane described by Warner and others (1989) in terms of their rock types and bulk-rock geochemistry.

SAMPLES

Due to poor SSR rock outcrops, samples of SSR rocks were collected from road cuts and construction sites in the southeastern part of Atlanta, Georgia (Figure 2). In this intense weathering environment, only the most resistant rocks remain even in deep road cuts or in construction foundations. Rocks of the SSR include amphibolites and diablastites composed of variable amounts of amphibole, chlorite, magnetite, and talc.

Samples were collected from four different parts of the SSR: Brittany Park Lane (BPL1, BPL2), Moore Road (Moore1, Moore3), West Side Place (West1, West2), and Wildcat Road (Wcat1, Wcat2) (Figure 2). Shown in Figure 3 is an outcrop of a megacrystic meta-orthopyroxenite from Wildcat Road, one of the best exposures of the SSR encountered. The sample shown in Figure 3 is composed of megacrystic euhedral brown crystals of orthopyroxene, altering to amphibole in places, set within fine-grained amphibole grains. Relict orthopyroxene grains are visible even in hand specimen.

METHODS

Thin sections were prepared from all of the samples collected for this study. Petrographic examination yielded mineral assemblages and textural relationships. The mode is the mineralogical composition of a rock (e.g., Philpotts, 1990) and it is expressed in volume percent. Mineral modes were obtained using point counting under the petrographic microscope, together with the use of a Clay Adams Laboratory Counter. A total of 500 counts were performed per thin section. Point counting results from the present study are shown Table 1. Mineral modes are important is classification of rocks as the IUGS classification scheme is based on volume percentages (Streckeisen, 1976).

Approximately 10.0 grams of the rock powder was weighed and mixed with 2 ml of acetone/elvalcite solution to produce powder pellets through applying a pressure of 21, 000 kPa. Trace element analyses were then made on the pressed powder pellets at the University of Georgia Center for Applied Isotope Studies on a Philips 2.4 kW Magix instrument. The instru-

Table 1. Mineral modes for samples from the Soapstone Ridge complex studied

Sample	BPL1	BPL2	Moore1	Moore3	West1	West2	WCAT	WCAT2
Amphibole	79.0	78.6	99.6	99.2	97.4	98.4	96.6	38.8
Chlorite	13.4	16.2	0	0	2.4	1.4	0	0
Talc	0	0	0	0	0	0	0.6	1.2
Opaques	7	4.8	0.4	0.8	0	0.2	1.4	0.4
Other*	0.6	0.40	0	0	0.2	tr	1.4†	59.6†

*Other – includes pits in thin sections and some accessory minerals such as apatite or as indicated †-orthopyroxene

ment is equipped with an Rh anode and a sequential spectrometer and the power settings varied according to the element of interest. Data obtained were corrected for peak overlaps and mass absorption effects. The analytical lines used were Kα with the exception of Ba, Hf, U, and Th, for which the Lα analytical line was used.

Major element analyses were carried out on fused glass disks following a slight modification of the method of Norrish and Hutton (1969). Approximately 10.00 g of lithium borate-lithium bromide fusion flux was weighed and added to approximately 2.50 g of sample to produce fused glass disks. The disks were analyzed utilizing the same instrument as was used for trace elements and data were corrected for peak overlap and mass absorption effects. Replicate analyses of standards indicated precisions of ± 1% (1 S.D.) for most major and trace elements.

The oxidized character of the SSR rocks is probably related to the weathering, hydration, alteration, and metamorphism of these rocks. Since normative mineralogy is sensitive to the oxidation state of the iron (e.g., Rollinson, 1993), the norms were all calculated following the assumption that 85% of the iron is Fe^{2+} (Cox and others, 1979). Rock analyses were recalculated to 100% anhydrous basis prior to both calculating the norms and plotting.

MINERALOGY AND PETROLOGY

Talc-chlorite amphibole schists are the most common rock types in our suite of SSR samples. Nonfeldspathic rocks of the SSR are grayish-green, where fresh, but weather to a brownish-gray color. The rocks contain coarse-grained amphibole crystals that are slightly more resistant to weathering than the associated chlorite and talc, giving the weathered rock a "knobby" appearance. The rocks are typically massive, but where a foliation is detected, it is the talc and chlorite that are responsible for the foliation.

Mineral modes in our SSR rocks are given in Table 1. Amphibole is the dominant mineral in SSR rocks, with the exception of one megacrystic meta-orthopyroxenite sample from Wildcat Road where orthopyroxene comprises at least 70% of the mode (Table 1). It can be seen from Table 1 that most of the rocks types are dominated by modal amphibole, and hence the use of CIPW norms in classifying rocks from the present investigation.

Brittany Park Lane and West side Place samples are composed mostly of amphibole and chlorite with minor amounts of FeTi oxide minerals (Table 1). Moore Road and Wildcat Road samples have hornblende overgrown by actinolite, no chlorite, and very few or no FeTi oxides (Table 1).

Amphiboles from Moore Road, West Side Place, and Brittany Park Lane samples are medium- to fine-grained and acicular. Individual, optically continuous amphibole grains range in size from 0.2 to 1.0 mm in length. Under the microscope, high-Ca amphibole is generally colorless, but a few grains contain patches of amphibole with slight greenish pleochroism. Low-Ca amphibole forms more elongate grains, often as overgrowths on high-Ca amphibole. Amphibole grains are enclosed by chlorite and talc. Chlorite is pleochroic (light-green to colorless) and talc is colorless. Small grains of magnetite, often oxidized to goethite, occur in Moore Road and West Side Place, and Brittany Park Lane samples. Blake (1982) reported that the amphiboles in SSR rocks were tremolite and cummingtonite.

In addition to the occurrence of acicular amphiboles, samples from Brittany Park Lane are also dominated by both fine- to medium-grained chlorite and very coarse-grained amphibole crystals. The coarse amphibole grains commonly enclose fine-grained opaque minerals. Zoned amphiboles, with hornblende cores discontinuously rimmed by tremolite-actinolite, are common in samples from Moore Road and West Side Place.

Wildcat Road samples (Figure 3) are dominantly composed of megacrystic grains of orthopyroxenes partially rimmed by, or occurring in association with, amphibole. Samples from Wildcat Road are different from the other SSR samples investigated in that they are the only orthopyroxene-bearing ones, in addition to am-

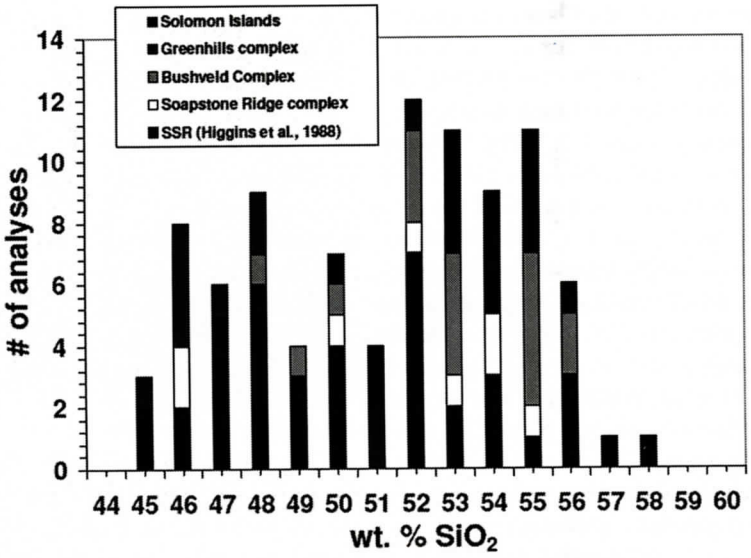

Figure 4. Bar diagram showing silica contents of samples from Higgins and others (1988) and samples from the present study. Smartville complex samples are shown for comparison purposes. Data from various a famous layered intrusion such as the Bushveld Complex (Maier and others, 2000) and island arc crust such as Solomon Islands (Berly and others, 2006) and Greenhills Complex (Spandler and others, 2003) are shown for comparison.

phibole, talc, and opaques. The orthopyroxene crystals in sample Wcat2 are very coarse-grained, sometimes up to 5 cm in length. Amphibole typically occurs in association with orthopyroxene, but the grain size of the former rarely exceeds 2mm in length, and the amphibole typically partially rims or replaces orthopyroxene crystals. Talc in Wildcat Road samples occurs in association with the amphiboles. Ortho-amphiboles were only identified in Wildcat Road samples, and these occur in association with orthopyroxenes. Sample Wcat is mostly comprised of amphibole replacing orthopyroxene; very few relict orthopyroxene grains were observed.

BULK COMPOSITIONS

Bulk-rock major and trace element composition data, including normative compositions, of 8 samples are reported in Table 2. In all the accompanying plots, samples from the present study are compared to those from Higgins and others (1988) and they are all described together. Rocks can be classified in terms of their silica content into ultrabasic, basic, and acid groups (e.g., Philpotts, 1990). A plot of the silica content of the rocks under study and those from Higgins and others (1988) is presented as a bar diagram (Figure 4) and it shows that the bulk of rocks from the SSR are basic and intermediate rocks.

On a plot of the oxide magnesia versus calcium oxide (Figure 5a), SSR rocks from the present investigation separate into two groups. One group has relatively low CaO contents which range from 3.01 wt.% to 4.23 wt.% CaO for five samples, whereas the other group of samples has relatively high CaO contents ranging from 6.27 – 8.39 wt.% CaO (Figure 5a). Except for the high modal calcic amphiboles in one sample with the highest CaO content (Moore3), it is not clear why this one sample has a much higher CaO content compared to the other samples. The other two samples with high CaO contents are from the Wildcat Road area, and they are composed of megacrystic orthopyroxenite with high modal amphiboles. These SSR samples have magnesia contents ranging from a low of 19.73 wt.% in the sample with the highest CaO

Table 2. Bulk-rock major and trace element compositions and CIPW Norms of Rocks from the Soapstone Ridge complex

	West1	West2	Moore1	Moore3	BPL1	BPL2	WCAT	WCAT2
SiO2	52.65	53.1	53.58	52.35	43.7	43.86	48.49	51.50
TiO2	0.24	0.21	0.35	0.77	0.53	0.59	0.33	0.32
Al2O3	5.48	4.54	3.76	5.28	7.33	7.96	6.46	5.23
$Fe_2O_3^t$	11.06	10.93	10.69	11.48	11.83	11.43	12.43	12.44
MnO	0.19	0.19	0.19	0.21	0.18	0.19	0.25	0.23
MgO	24.49	25.12	25.51	19.73	27.78	26.76	21.63	22.89
CaO	3.01	3.21	3.35	8.39	3.43	4.23	7.64	6.27
Na2O	0.21	0.24	0.10	0.58	0.18	0.04	0.66	0.60
K2O	0.04	0.05	0.06	0.10	0.06	0.04	0.07	0.11
P2O5	0.02	0.02	0.10	0.11	0.04	0.06	0.01	0.02
LOI	3.95	3.29	3.19	1.61	6.30	6.11	1.69	0.54
Total	101.34	100.90	100.88	100.60	101.36	101.27	99.65	100.15
FeO*	11.33	11.17	10.92	11.57	12.42	11.99	12.56	12.36
	Normative compositions							
quartz	1	2	2	0	0	0	0	0
corundum	0	0	0	0	1	0	0	0
orthoclase	0	0	0	1	0	0	0	1
albite	2	2	1	5	2	0	6	5
anorthite	14	11	10	12	18	22	15	11
diopside	1	4	5	24	0	0	19	16
hypersthene	86	79	79	55	38	40	37	53
olivine	0	0	0	0	38	35	21	11
magnetite	2	2	2	2	2	2	2	2
ilmenite	0	0	0	1	1	1	1	0
apatite	0	0	0	0	0	0	0	0
	Trace elements (in ppm)							
	West1	West2	Moore1	Moore3	BPL1	BPL2	Wcat	Wcat2
V	97	84	94	173	76	78	141	119
Ni	838	694	638	577	809	1049	771	853
Cr	1534	2293	1926	1344	2685	2392	1891	1881
Cu	14	20	21	13	25	21	20	47
Zn	148	138	125	143	137	160	153	177
Rb	8	8	8	8	9	9	9	8
Sr	bdl	22	14	39	60	27	bdl	bdl
Y	4	7	6	16	7	13	13	23
Zr	13	15	23	36	50	44	20	23
Nb	1	1	3	3	3	3	1	bdl
Ba	bdl	12	45	bdl	bdl	bdl	69	68
Ce	88	88	90	84	89	94	nd	nd
La	3	25	3	18	5	11	9	14

*Iron partitioned based on ratios of Fe^{2+}/Fe^{3+} = 0.85 (Cox and others, 1979); ^{t} - total iron as Fe_2O_3, bdl – below detection limit, nd – not determined.

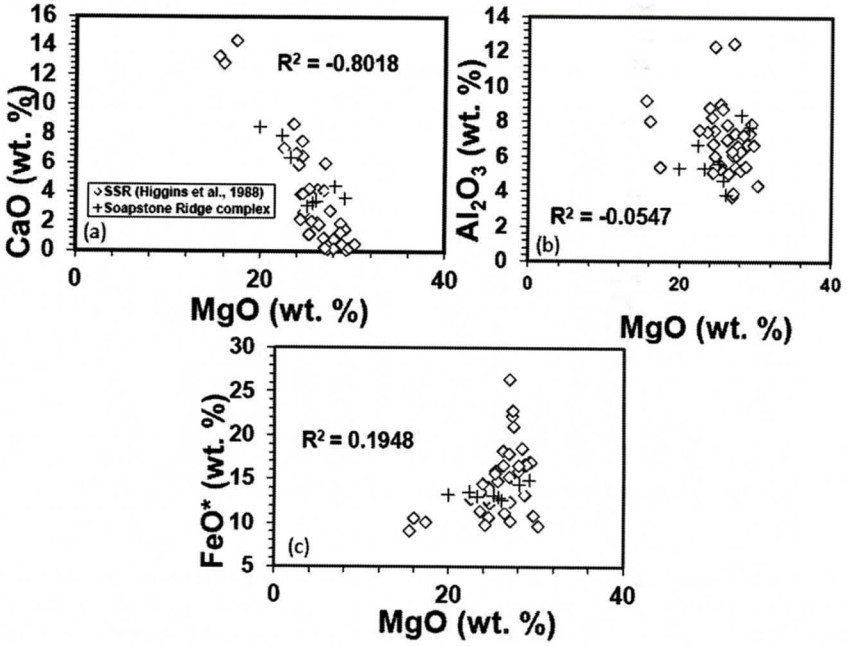

Figure 5. Plot of wt.% MgO *versus* wt.% CaO (a), wt.% Al_2O_3 (b), and total iron as wt.% FeO^* (c). Only CaO versus MgO shows a negative correlation, the other elements do not display any correlation.

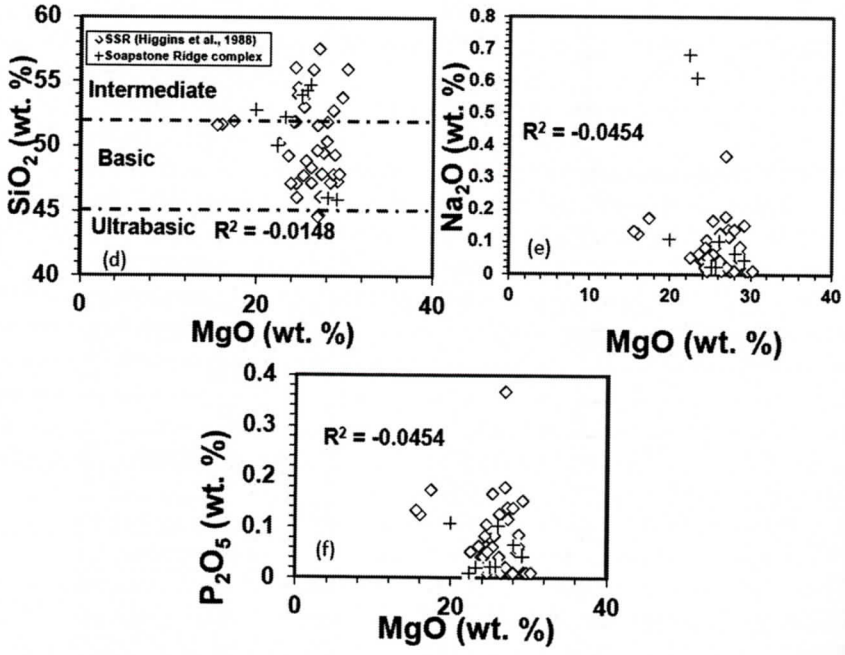

Figure 5 (continued). Plot of wt.% MgO *versus* wt.% SiO_2 (d), wt.% Na_2O (e), and wt.% P_2O_5 (f), wt. %. No correlation is displayed by these elements.

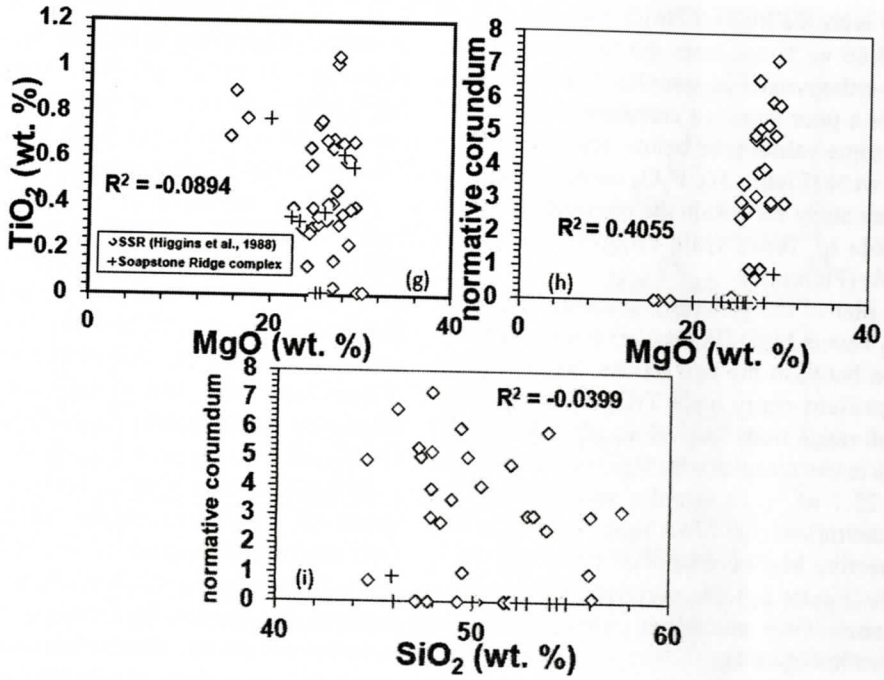

Figure 5 (continued). Plot of wt.% MgO *versus* wt.% wt.% TiO_2 (g), % normative corundum versus wt.% MgO (h), and % normative corundum versus wt.% SiO_2 (i).

content (Moore3) to a high of 27.78 wt.% in a sample with a relatively low CaO content (BPL1) as shown in Figure 5a. The range displayed by samples from the present study is comparable to and plots within the range of samples from Higgins and others (1988) (Figure 5a). As MgO contents decrease, CaO contents increase, resulting in a good negative correlation that is displayed between these two oxides (Figure 5a). The MgO contents of SSR samples from the present study fall within the MgO range of 15.2 – 28.5 wt.% from Higgins and others (1988) (Figure 5a).

All of the SSR present samples are moderately aluminous with aluminum oxide contents ranging from a low of 3.76 wt.% Al_2O_3 (sample Moore1) to a high of 7.96 wt.% Al_2O_3 (sample BPL2) as shown in Figure 5b. These samples are comparable to, and they fall within, the 3.52-11.7 wt.% Al_2O_3 range from the data of Higgins and others (1988) (Figure 5b). No correlation is displayed between Al_2O_3 and MgO as shown in Figure 5b.

Iron contents are high and total iron (as FeO*) contents do not correlate with MgO contents (Figure 5c). Samples with low FeO* contents are also characterized by samples with low MgO contents, but the relationship breaks down as the concentrations of both oxides increase (Figure 5c). FeO* contents from the present study show a limited range, varying from 10.92 - 12.56 wt.%, and they plot within the range of Higgins and others (1988) (Figure 5c). FeO* data from Higgins and others (1988) show a wider range from 8.14-20.05 wt.% (Figure 5c).

No correlation is displayed in a plot of SiO_2 versus MgO (Figure 5d). In Figure 5d, SiO_2 contents from SSR samples under study range from 43.7-52.65 wt.% and they plot completely within the 42.0-54.5 wt.% range from Higgins and others (1988). Almost all of the samples from the SSR plot in the basic and intermediate field (e.g., Philpotts, 1990).

Alkali contents are low, $Na_2O < 1$ wt% for all samples (Figure 5e), and approximately a fifth of K_2O values from the data of Higgins and others (1988) fall at or below detection limits. In Figure 5e, the two samples from the present

study with the highest Na_2O contents of 0.58 and 0.66 wt.% are from the two megacrystic meta-orthopyroxenite samples. The oxide P_2O_5 shows a poor negative correlation with MgO, with some values at or below detection limit of 0.01 wt.% (Figure 5f). P_2O_5 contents from the present study are within the range of, and comparable to, those from Higgins and others (1988) (Figure 5f).

A plot of the generally incompatible oxide TiO_2 *versus* MgO (Figure 5g) shows no correlation between the two oxides. Samples from the present study have TiO_2 concentrations which range from low values of 0.24 and 0.21 wt.% in two samples with MgO contents of 25.1 and 25.7 wt.%, to samples with higher TiO_2 concentrations of 0.77 wt.% and 0.59 wt.% with respective MgO contents of 19.73 and 26.76 wt.% (Figure 5g). No correlation is displayed between TiO_2 and MgO concentrations as shown in Figure 5g.

Figure 5h is a plot of normative corundum versus wt.% MgO that shows that approximately half of the samples from the SSR analyzed by Higgins and others (1988) have normative contents of >1%. Normative igneous mineralogies for the SSR rocks range from silica over-saturated rocks (normative quartz) to silica saturated rocks (normative olivine). The rocks contain appreciable normative plagioclase compared to their moderate aluminum contents. There is an excess of Al (insufficient Ca+Na+K) in many of the rocks resulting in corundum in the norm (Figure 4h). To evaluate whether there is a correlation between normative corundum and wt.% SiO_2, a plot of the two shown in Figure 5i shows that no correlation is displayed in this diagram. Except for the oxides CaO *versus* MgO, the mostly basic rocks of SSR show little inter-element correlation (Figure 5). Typical igneous variation diagrams designed to show fractionation trends show considerable scatter in the SSR data with little, if any, correlation (except the CaO-MgO plot). Amphiboles, chlorite, and talc are the common mineral phases and this is reflected in LOI's that are typically in the range of 5 to 7 wt%.

Chromium, a highly compatible element in basaltic magmas, ranges from high values of over 3000 ppm in samples with > 27 wt.% MgO to values of approximately 1300 ppm in samples with < 23 wt.% MgO (Figure 6a), displaying a very weak positive correlation for data from Higgins and others (1988) but a good positive correlation for data from the present study.

Nickel, another highly compatible element in basaltic magmas, is plotted versus the oxide MgO in Figure 6b. Nickel concentrations vary from values of over 1200 ppm in samples with MgO values in excess of 27 wt% to a values 270 ppm in a sample with value of 15.5 wt.% MgO (Figure 6b). A very weak positive correlation is displayed by both data from Higgins et al (1988) and from the present study (Figure 6b).

In melts, if bulk igneous compositions are preserved, Cu concentrations should increase with decreasing MgO which should be consistent with the behavior of a broadly incompatible element. In cumulate rocks, however, this behavior is not always clearly defined due to the occurrence of pockets of trapped intercumulus liquid. In the rocks under investigation, Cu contents range from values of less than 10 ppm to values as high as 200 ppm, but display no correlation when plotted versus magnesium (Figure 6c). A very weak positive correlation is displayed by both data sets plotted in Figure 6c.

Vanadium is commonly concentrated in magnetite and hornblende, to a lesser degree in clinopyroxene and plagioclase (e.g., Frey and others, 1978; Hart and Dunn, 1993; Rollinson, 1993). In samples from the SSR, V concentrations range from values at below detection limit to values of approximately 80 ppm (Figure 6d). No correlation exists between V and MgO for data from Higgins et al (1988), although a strong negative correlation is displayed by data from the present study (Figure 6d).

Zirconium is a cation that is excluded from common rock-forming minerals although it is concentrated in zircon, and can substitute in Fe-Ti oxides (e.g., Pearce and Norry, 1979; Hess, 1989). Zirconium concentrations in the SSR show a wide range from values at or below detection limit to values close to 300ppm (Figure 6e). Zr contents from both data sets display no correlation when plotted versus MgO (Figure 6e).

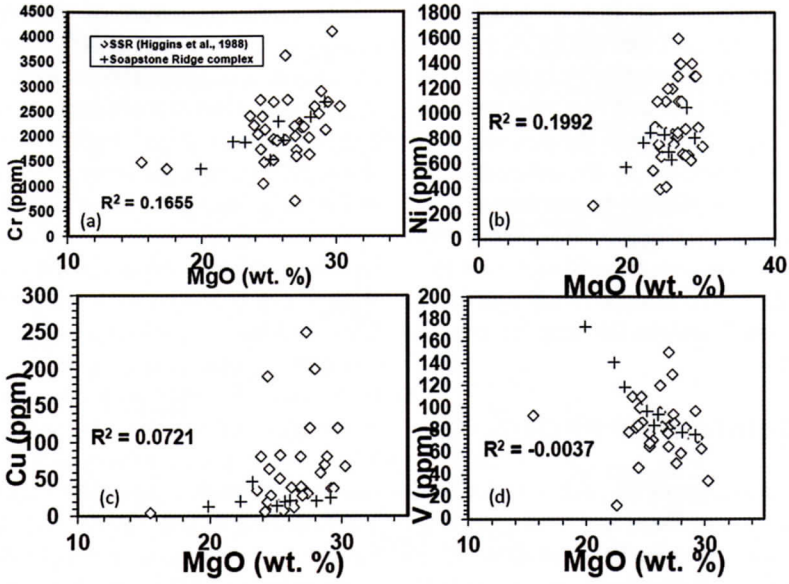

Figure 6. Plot showing wt.% MgO *versus* compatible trace elements ppm Cr (a) and ppm Ni (b). The high Ni and Cr concentrations shown are an indication of the cumulate nature of Soapstone Ridge complex rocks. (c) and (d) show, respectively, ppm Cu and ppm V concentrations plotted *versus* wt.% MgO.

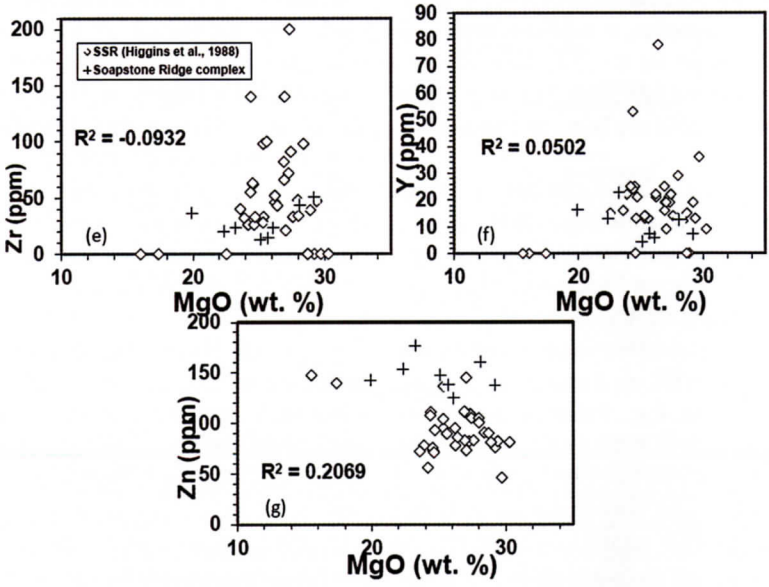

Figure 6 (continued). Plot showing wt.% MgO *versus* trace elements Zr (e), Y (f), and Zn (g) concentrations, in ppm. No correlations are displayed by these plots.

Yttrium, an incompatible element in mafic magmas and a proxy for the rare earth elements, has concentrations in the SSR ranging from below detection limit to concentrations of ~80 ppm (Figure 6f). There is no correlation displayed between Y and MgO for both data sets which are comparable (Figure 6f).

Zinc is excluded from both ortho- and clinopyroxene, and plagioclase (Cox and others, 1979) but it can be concentrated in olivine

(Paster and others, 1974). In SSR samples, Zn concentrations range from values of approximately 40 ppm to values of ~180 ppm with no correlation between Zn and MgO for both data sets (Figure 6g). Data from the present study tend to be characterized by Zn concentrations which are generally slightly higher than or comparable to, data from Higgins and others (1988) (Figure 6g). Again, megacrystic meta-orthopyroxenite samples and sample BPL2 contain the highest Zn concentrations for samples from the present study.

DETERMINATION OF PROTOLITHS

Bulk compositions of 39 rock samples from Higgins and others (1988) and 8 samples from the present study from the SSR are all shown in Figures 4 and 5 and they have anhydrous SiO_2 values ranging 45 to 58 wt.%. They range in composition from ultrabasic (44.6 and 44.9 wt%; only 2 samples as shown Figure 5d), through basic (45.9 – 51.9 wt.%; comprising the bulk of the rock samples, n = 35) to intermediate (52.8 – 57. 6 wt.%; n = 10 samples) bulk compositions (Figure 5d). Thus, the majority of the rocks from the SSR are basic and intermediate rocks.

It has been shown that rocks derived from melting of the upper mantle have rather restricted ranges in their major element contents such as Al_2O_3 and CaO *versus* MgO (e.g., Figures 7a and b). A plot of the Al_2O_3 *versus* MgO shows bulk-rock geochemical variations for all the samples from the SSR on a cumulate triangle diagram (Figure 7a, e.g., Peterson and Ryan, 2009). Another plot of CaO *versus* MgO (Figure 7b) shows that SSR samples are comprised of orthopyroxene- and clinopyroxene-rich and relatively olivine-rich cumulates compared to melts such as mid-ocean ridge basalts (MORB). On a plot of CaO *versus* MgO, the cumulate nature of SSR rocks is noticeable as these rocks are enriched in orthopyroxene compared to MORB and komatiites (Figure 7b). Komatiites, which are MgO-rich lavas, are only comparable to a few samples from the SSR (Figure 7). The majority of SSR samples are enriched in orthopyroxene compared to komatiites.

The cumulate nature of SSR rocks is also demonstrated on a plot of Ni *versus* MgO (Figure 8). Nickel concentrations from the SSR are much higher than those of melts such as MORB and tholeiites, and such high Ni concentrations shown in Figure 8 are a result of olivine accumulation for which Ni has a high affinity.

Plutons which underlie volcanic arcs in island arc settings form the island arc crust (e.g., Winter, 2010). Pyroxenites and gabbroic cumulates predominate rocks types typically encountered in arc crustal segments, and peridotites form relatively small proportions of rock types in arc crust settings (e.g., Spandler and others, 2003). Island arc cumulates such as those from Greenhills complex (Spandler and others, 2003) and Solomon Islands (Berly and others, 2006) have bulk-rock geochemical compositions comparable to SSR rocks (Figures 7a, b). The Marum ophiolite (an ocean floor ophiolite, e.g., Jaques and others, 1983) is characterized by wider ranges in MgO contents than those from SSR and other island arc complexes (e.g., Figure 8). This suggests that rocks ranging from olivine-rich cumulates (higher MgO contents) to basaltic rocks (lower MgO contents) are preserved in the Marum ophiolite compared to the SSR. It is thus here interpreted that the SSR has bulk-rock compositions that are more akin to those from island arcs than mid-ocean ridge-type cumulates such as the Samail ophiolite complex and layered intrusions as discussed later.

Ultramafic rocks from SSR are mostly meta-orthopyroxenites, and SSR mafic and intermediate rocks are meta-olivine gabbronorites, metagabbronorites. CIPW normative mineralogy for SSR samples is high in normative pyroxene, with minor to moderate amounts of normative plagioclase. Normative olivine and normative quartz occur in variable amounts. Mid-ocean ridge-type ophiolites such as the Samail ophiolite are characterized by rocks with much higher normative olivine contents than those from SSR samples (Figure 9). Comparison of the normative compositions of SSR rocks to rocks from ophiolites and island arcs shows that SSR rocks are depleted in normative plagioclase and enriched in normative pyrox-

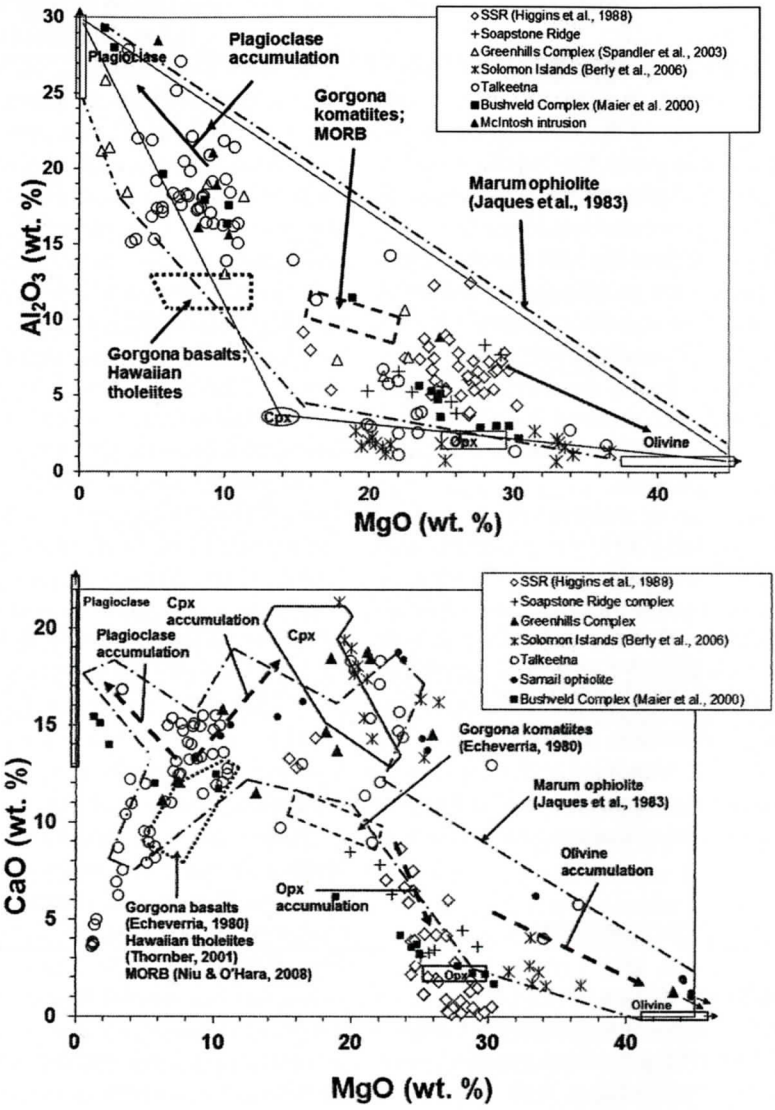

Figure 7 (a). Plot of Al_2O_3 *versus* MgO for samples from the study area. The cumulate triangle apices (e.g., Peterson and Ryan, 2009) are defined by olivine, plagioclase, and cpx (clinopyroxene) compositions from the SSR and Chaumba (2009). Fields for high-Mg melts such as komatiites and typical upper mantle melts such as tholeiites and basaltic komatiites are also shown. Mid-ocean ridge basalts (e.g., Frey and others, 1974) also plot in the Gorgona basalts field (Echeverria, 1980). Fields of Gorgona komatiites are from Echeverria (1980); plagioclase, olivine, cpx, and opx (orthopyroxene) after Bryan (1979), Frey and Clague (1983). McIntosh intrusion data are from Mathison and Hamlyn (1987). (b) Plot of CaO *versus* MgO for samples from the SSR. Fields for high-Mg melts such as komatiites and typical upper mantle melts such as tholeiites and basaltic komatiites are also shown. Mid-ocean ridge basalts (e.g., Frey and others, 1978) also plot in the Gorgona basalts field. Fields of plagioclase, olivine, cpx (clinopyroxene), and opx (orthopyroxene) after Bryan (1979), Frey and Clague (1983), and this work. The dashed line arrows represent the fractionation of olivine and orthopyroxene, followed by clinopyroxene (e.g., Garcia and others, 2003).

ene, a signature comparable to island arc cumulate rocks (Figure 9).

Given the presence of substantial amounts of normative corundum in some of the SSR samples, a likely cause of the elevated normative corundum (Al relative to Ca+Na+K) is loss of Ca, Na, and/or K during metamorphism and alteration. These processes would preferentially remove Na and K from the SSR samples. These two components are mobile during alteration and metamorphism under both amphibolite and greenschist facies conditions (e.g., Rollinson, 1993) as well as during weathering. Calcium appears to have been retained in calcic amphiboles, hence the negative correlation between calcium and magnesium.

Metamorphism or weathering would (and likely did) partially alter the protoliths rock chemistry prior to metamorphism. The observation that relict igneous trends are still observed in a plot of the oxides CaO and MgO is an indication that even though loss of some of the elements likely occurred during metamorphism, the data allow inferences to be made about the origin of the SSR. Removing SSR samples with normative corundum contents of >1% from the plots presented above does not alter the patterns shown.

DISCUSSION

The stable assemblages for SSR rocks appear to be chlorite + talc + cummingtonite + magnetite, consistent with a medium grade of metamorphism. Amphibolites in the SSR suite contain hornblende + plagioclase ± epidote, consistent with the amphibolite facies of regional metamorphism. Further quantification of metamorphic grade is beyond the scope of this paper. Even though ~50% of samples from Higgins and others (1988) contain normative corundum, the observation that if normative corundum bearing samples are removed doesn't change the observed trends is an indication that meaningful information can be obtained from these data.

Most of SSR samples described here are cumulates, as shown by the high concentrations of incompatible trace elements such as Ni (up to 1000 ppm) and Cr (up to 2600 ppm), and even high when including data from Higgins and others (1988). Basic magmas, such as mid-ocean ridge lavas, have low concentrations of Ni and Cr of approximately 100 ppm and 350 ppm (e.g., Wilson, 1989). High magnesia contents in some SSR samples in excess of 25 wt.% MgO also attest to the cumulate nature of the rocks under investigation, as magmas have typical MgO values of ~8 wt.% (e.g., Wilson, 1989). SSR MgO concentrations are less than 40 wt.%, which compares well with rocks which occur in subarc cumulates such as Talkeetna (e.g., Beyer, 1980; Greene and others, 2006; Rioux and others, 2007; Farris, 2009) (Figure 7).

Most of the samples from the present investigation have concentrations that are broadly comparable to those from Higgins and others (1988). A few notable exceptions occur, however, such as the relatively low concentrations of Zr and Y from the present study (e.g., Figures 6e, 6f) compared to those from Higgins and others (1988). The reasons for these dissonances could be due to the fewer number of samples from the present study compared to that from Higgins and others (1988). The other reason could be due to element calibration and/or interference in old XRF machines (possibly on which the Higgins and others (1988) data were analyzed) compared to modern ones (e.g., La Tour, 1987).

Over half of samples reported in Higgins and others (1988) contain normative corundum (Figures 5h, i). Unaltered cumulates from basic igneous rocks have little or negligible normative corundum contents (e.g., Best, 2003). Corundum appears in the norm where there is insufficient Ca, Na, and K to combine with the Al to form feldspar. The extremely low alkali contents and generally low Ca contents of the SSR rocks (Table 2) relative to Al result in normative corundum. Loss of alkalis and Ca is common during the weathering and/or alteration of mafic rocks (e.g., Cox and others, 1979; Schroeder and others 2000), and it is suggested that these corundum-normative basic rocks may reflect such compositional modification.

Based on normative mineralogy, only 2 samples from SSR are ultramafic, two of them plot

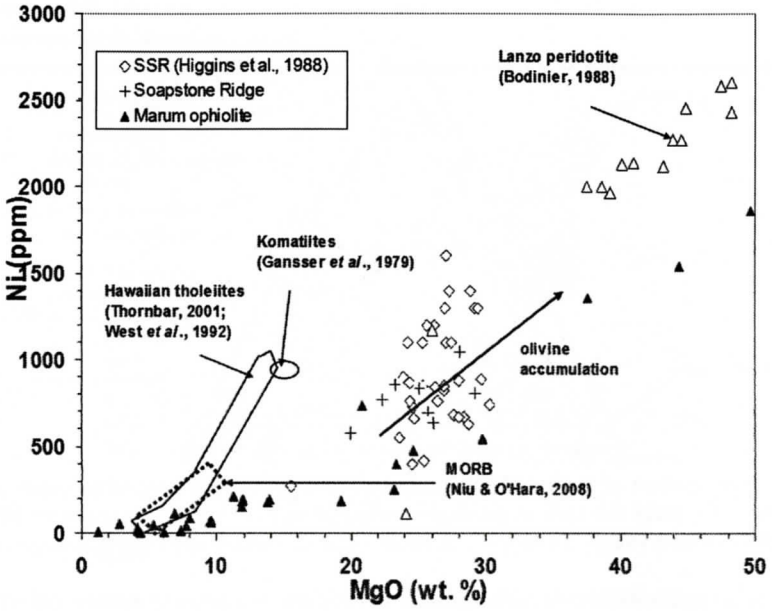

Figure 8. Plot of Ni *versus* MgO for samples from the SSR. Fields for high-Mg melts such komatiites and typical upper mantle melts such as tholeiites and basaltic komatiites are also shown. Field for normal mid-ocean ridge basalts (e.g., Schilling and others, 1983), Hawaiian tholeiites (Thornber, 2001; West and others, 1992) and Gorgona komatiites (Gansser and others, 1979) are also shown.

in the harzburgite field and a single sample plots in the field of olivine orthopyroxenite. The majority of rocks of the SSR plot in the fields of olivine gabbronorites, gabbronorites, and plagioclase-bearing ultramafic rocks (Figure 9). Many of the rocks plot near the pyroxene apex of the olivine-plagioclase-pyroxene gabbroic ternary classification diagram (Figure 9). Higgins and others (1988) refer to these rocks as pyroxenites. An examination of Figure 9, however, shows this to be not the case, as these rocks are mostly gabbroic with many having normative plagioclase contents over 10%. Normative olivine compositions are similarly low (< 45% in all SSR samples). SSR rocks, therefore, are dominantly mafic. Rocks from SSR are comparable to cumulate samples island arc complexes (e.g., Spandler and others, 2003), and pyroxenites from a supra-subduction zone, Solomon Islands (Berly and others 2006) (Figures 4, 7, 9). The best analogues for SSR samples are pyroxenites and gabbroic rocks from supra-subduction zones such as the Solomon Islands and Talkeetna arc (Figure 9). Samples from the Balkan-Carpathian ophiolite and from the Marum ophiolite are composed of rocks which range in composition from dunites through pyroxenites to olivine gabbros and gabbros (Savov and others, 2001; Jaques and others, 1983). SSR CIPW normative plagioclase contents, however, are not comparable to those from the Greenhills Complex. Samples from the present study contain no more than 22% normative plagioclase (albite + anorthite) compared to samples from the Greenhills Complex which have normative plagioclase contents in excess of 60% (Figure 9).

The SSR data provided (e.g., Figure 7) show that MgO contents from the SSR extend to relatively much lower MgO values (< 31 wt.%) compared to those from ophiolite complexes such as the Marum ophiolite. This observation is consistent with cumulate rocks derived from the highly differentiated nature of island arc magmas compared to normal mid-ocean ridge type magmas (Davidson, 1996). This highly differentiated nature probably resulted in less olivine-bearing rocks in the SSR and in the

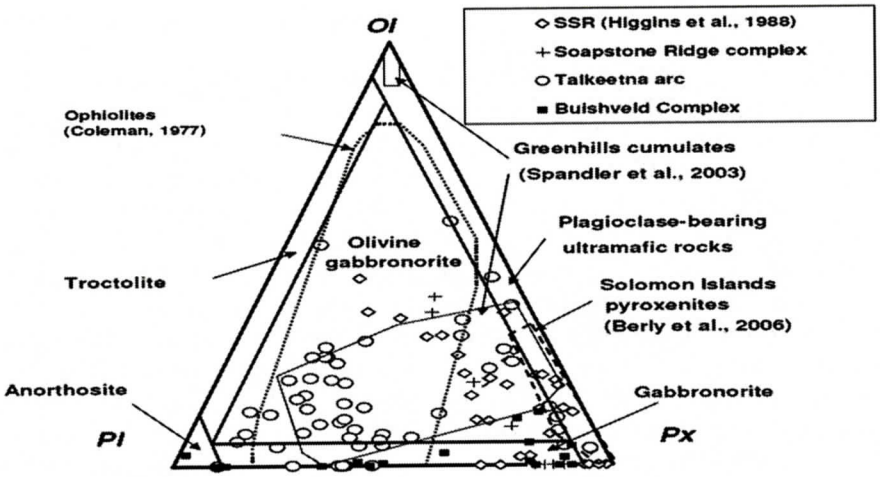

Figure 9. Comparison of the normative compositions of the SSR rocks to rocks from ophiolites and island arcs. Note the lack of normative plagioclase contents in excess of 37% for samples from the Soapstone Ridge complex. Abbreviations: Ol – olivine; Pl – plagioclase; Px – pyroxene.

abundant metapyroxenites and metagabbros observed. Other intra-oceanic island arcs such as the Talkeetna arc are also characterized by abundant metagabbroic rocks (Figure 7).

If SSR originated as an intra-oceanic arc, it has implications on the tectonic evolution of the southern Appalachians. Current models for the evolution of the southern Appalachians involve various lithotectonic terranes such as the Tugaloo and Cat Square terranes, as well as the Carolina superterrane which were outboard of the Laurentia (Iapetan and peri-Gondwanan Realm) during the closing of the proto Atlantic (Iapetus) ocean (e.g., Hibbard and others, 2002, 2006;; Hatcher and others, 2007). These terranes were then accreted to the Laurentia during the final stages of the formation of Pangea (Hatcher and others, 2007). These models, however, make no mention of the SSR and similar cumulate rocks in the southern Appalachian Piedmont.

A model based upon the one provided by Hatcher and others (2007) but requiring modifications to accommodate the SSR and similar rocks is here proposed. A plausible model for the origin of the SSR and the southern Appalachians envisages the SSR (and possibly other comparable metamorphosed mafic and ultramafic bodies in the Iapetan and peri-Gondwanan Realm) as an intra-oceanic island arc(s) which was present between the Tugaloo terrane and the Carolina superterrane (Figure 10a). With continued closure of the Iapetus Ocean, some of the island arcs probably first collided against each other, metamorphosing the SSR under amphibolite facies conditions (Figure 10b). During the final stages of the formation of Pangea, the SSR was then thrusted onto its present position in the Tugaloo terrane due to thrusting of the SSR towards Laurentia, accompanied by greenschist facies metamorphism (Figure 10b). Other rock types which initially overlain the SSR cumulate pile have probably since been eroded away (e.g., Allard and Whitney, 1994). The original setting of the original island arc which later formed the SSR is envisaged to have been originally formed either between the Tugaloo terrane and the Carolina superterrane, and it was later thrusted onto the Tugaloo terrane during the final stages of the assembly of Pangea (Figures 10a, b).

CONCLUSIONS

Plots of bulk-rock geochemistry of the SSR samples do not show well-defined trends, in part due to the cumulate origin of the rocks, and also probably due to the metamorphism which affected these rocks. Many SSR rocks contain normative corundum, which is not common in

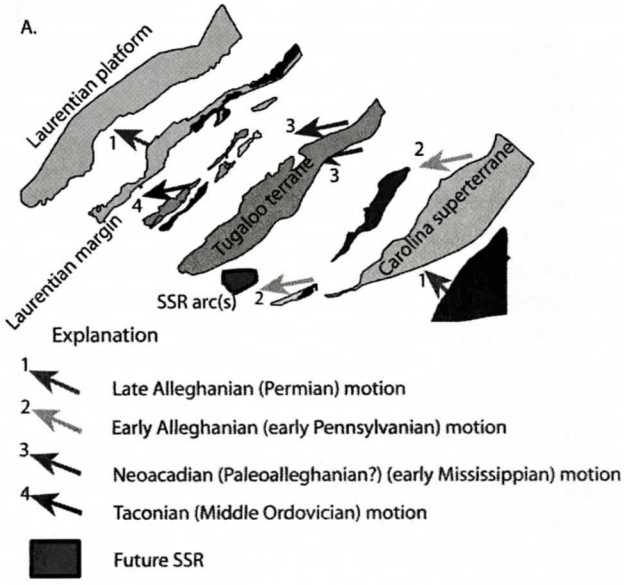

Figure 10a. Retrodeformed tectonostratigraphic terranes in the southern Appalachians with arrows indicating broad kinematics of assembly. Arrows shown are color-coded to show accretion timing (after Hatcher and others, 2007).

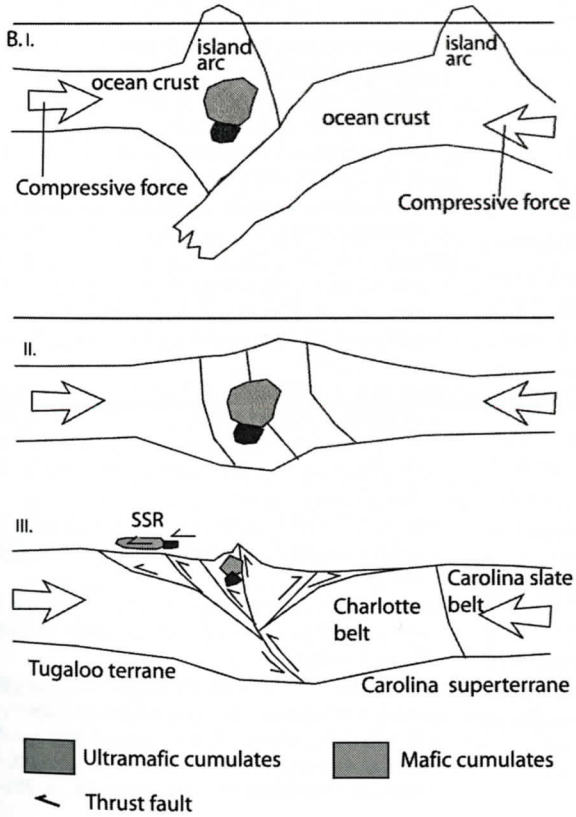

Figure 10b. Cartoon illustrating the envisaged events that led to development of the SSR. A. Arc-arc collision during initial stages of the assembly of Pangea, B. Metamorphism of the SSR resulting from arc-arc collision and thrusting of the SSR onto Tugaloo terrane due to collision of various arcs during final assembly of Pangea in stages indicated as i., ii., and iii.

unaltered mafic igneous rocks, indicating chemical altering of some of these samples. However, some conclusions can be drawn from the bulk-rock geochemistry of the SSR rocks as some of the samples have little or negligible normative corundum contents.

SSR rocks are mostly comprised of metapyroxenites and metagabbros which are comparable to those from intra-oceanic arc cumulates, such as the Solomon Islands (Berly and others, 2006) and the Greenhills complex in New Zealand (Spandler and others, 2003). The paucity of peridotitic cumulates and the predominance of pyroxenitic and gabbroic cumulates in the SSR may indicate that the SSR was probably formed in an island arc setting, from mantle wedge melting above a subducting slab which was contaminated by fluids derived from a subducting oceanic slab (e.g., Wilson, 1989; Grove and others, 2006). Due to the similarities of the SSR to some metamorphosed mafic and ultramafic rocks in the Tugaloo terrane of the southern Appalachian in terms of their component rock types, petrography, bulk-rock geochemistry, and mineral compositions, one could imply that some of these bodies probably also originated as island arc crustal segments.

ACKNOWLEDGEMENTS

Mike Higgins and Ralph Crawford are thanked for showing the author the Soapstone Ridge complex exposures and also for discussions on southern Appalachians geology. Mike Roden helped with some of the fieldwork on the SSR. A very thorough and helpful review by an anonymous review improved the manuscript and it is gratefully acknowledged. Sam Swanson is credited with getting this work started, and offered helpful ideas. Critical reviews before submission of the article by Sam Swanson, Loren Raymond, Mike Roden, and Richard Warner greatly improved the manuscript and they are gratefully acknowledged. Funding from Watts-Wheeler and the Allard Award, University of Georgia, and a GSA student research grant helped cover some of the costs of this research.

REFERENCES

Allard, G.O. and Whitney, J.A., 1994, *Geology of the Inner Piedmont, Carolina Terrane, and Modoc Zone in Northeastern Georgia*, Georgia Geological Survey, Project Report 20, 36 p.

Allard, G. and Whitney, J., 1995, The Russell Lake Allochthon – a neglected tectonostratigraphic unit in the southern Appalachians, *South Carolina Geology*, v. 38, p. 71-77.

Berly, T.J., Hermann, J., Arculus, R.J. and Lapierre, H., 2006, Supra-subduction zone pyroxenites from San Jorge and Santa Isabel (Solomon Islands), *Journal of Petrology*, v. 47, p. 1531-1555.

Best, M.G., 2003, *Igneous and Metamorphic petrology*, Blackwell, Maden, Massachussetts, 729 p.

Beyer, B.J., 1980, *Petrology and geochemistry of ophiolite segments in a tectonic mélange, Kodiak Islands, Alaska*, Unpublished Ph.D. thesis, University of California, Santa Cruz, 227 p.

Blake, R.L., 1982, Amphiboles of the Soapstone Ridge, Ga, United States Department of the Interior, Bureau of Mines, Report of Investigation 8627, 17p.

Bodinier, J.L., 1988, Geochemistry and petrogenesis of the Lanzo peridotite body, western Alps, *Tectonophysics*, v. 149, p. 67-88.

Bream, B.R., Hatcher, R.D., Jr., Miller, C.F. and Fullagar, P.D., 2004, Detrital zircon ages and Nd isotopic data from the southern Appalachian crystalline core, Georgia, South Carolina, North Carolina, and Tennessee: new provenance constrains for part of the Laurentian margin, in Tollo, R.P., Corriveau, L., McLelland, J. and Bartholomew, M.J. (eds.) *Proterozoic tectonic evolution of the Grenville orogen in North America*, Geological Society of America Memoir 197, p. 459-475.

Bryan, W.B., 1979, Regional variation and petrogenesis of basalt glasses from the FAMOUS area, Mid-Atlantic Ridge, *Journal of Petrology*, v. 20, p. 293-325.

Chaumba, J.B., 2009, *The Russell Lake Allochthon, Southern Appalachians: structure, petrography, bulk-rock and mineral chemistry, O, H, and Sm-Nd isotope geochemistry*, Ph.D. Dissertation, University of Georgia, Athens, 390 p.

Chaumba, J.B. and Roden, M.F., 2007, Structural setting and mineral compositional data from the Durhamtown mafic complex, east central Georgia (abs), *Geological Society of America Abstracts with Programs*, v. 39, no. 2, p. 27.

Coleman, R.G., 1977, *Ophiolites – Ancient Oceanic Lithosphere?*, Minerals and Rocks, v. 12, Springer-Verlag, 229 p.

Cox, K.G., Bell. J.D. and Pankhurst, R.J., 1979, *The interpretation of igneous rocks*, George Allen and Unwin, London, 450 p.

Davidson, J.P., 1996, Deciphering mantle and crustal signatures in subduction zone magmatism, in: Bebout, G.E., Scholl, D.W., Kirby, S.H. and Platt, J.P. (eds.), *Subduction to bottom*, American Geophysical Union, Geophysical Monograph 96, Washington, DC, p. 251-262.

Echeverria, L.M., 1980, Tertiary or Mesozoic komatiites from Gorgona island, Columbia: field relations and geochemistry, *Contributions to Mineralogy and Petrology*, v. 73, p. 253-266.

Farris, D.W., 2009, Construction and evolution of the Kodiak Talkeetna arc crustal section, southern Alaska, in: Miller, R.B. and Snoke, A.W. (eds.), *Crustal cross sections from the western North American cordillera and elsewhere: implications for tectonic and petrologic processes*, Geological Society of America, Special Publication 456, p. 69-96.

Frey, F.A., Green, D.H. and Roy, S.D., 1978, Integrated models of basalt petrogenesis: a study of quartz tholeiites to olivine melilitites from southeastern Australia utilizing geochemical and experimental petrological data, *Journal of Petrology*, v. 19, p. 463-515.

Frey, F.A. and Clague, D.A., 1983, Geochemistry of diverse basalt types from Loihi Seamount, Hawaii: petrogenetic implications, *Earth and Planetary Science Letters*, v. 66, p. 337-355.

Gansser, A., Dietrich, V.J. and Cameron, W.E., 1979, Palaeogene komatiites from Gorgona Island, *Nature*, v. 278, p. 545-546.

Garcia, M.O., Pietruszka, A.J, and Rhodes, J.M., 2003, A petrologic perspective of Kilauea volcano's summit magma reservoir, *Journal of Petrology*, v. 44, p. 2313-2339.

Greene, A.R., DeBari, S.M., Kelemen, P.B., Blusztajn, J. and Clift, P.D., 2006, A detailed geochemical study of island crust: the Talkeetna arc section, south-central Alaska, *Journal of Petrology*, v. 47, p. 1051-1093.

Grove, T.L., Chatterjee, N., Parman, S.W. and Médard, E., 2006, The influence of H_2O on mantle wedge melting, *Earth and Planetary Science Letters*, v. 249, p. 74-89.

Hart, S.R. and Dunn, T., 1993, Experimental cpx/melt partitioning of 24 trace elements, *Contributions to Mineralogy and Petrology*, v. 113, p. 1-8.

Hatcher, R.D., Jr., Merschat A.J. and Thigpen, J.R., 2005, Blue Ridge primer, in Hatcher, R.D., Jr. and Merschat, A.J. (eds.) Blue Ridge geology geotraverse east of the Great Smoky Mountains National Park, western North Carolina, *Carolina Geological Society Guidebooks*, p. 1-24.

Hatcher, R.D., Bream, B.R. and Mershat, A.J., 2007, Tectonic map of the southern and central Appalachians: a tale of three orogens and a complete Wilson cycle, in: *4-D framework of continental crust, Geological Society of America*, Boulder, Colorado, Memoir 200, p. 595-632.

Hess, H.H., 1955, Serpentinites, orogeny and epeirogeny, *in* Poldervaart, A. (ed), *Crust of the Earth*, Geological Society of America Special Paper 62, p. 391-408.

Hess, P.C., 1989, *Origin of igneous rocks*, Harvard University Press, Cambridge, MA, 336 p.

Hibbard, J.P., Stoddard, E.F., Secor, D.T. and Dennis, A.J., 2002, The Carolina Zone: overview of Neoproterozoic to early Paleozoic peri-Gondwana terranes along the eastern flank of the southern Appalachians, *Earth-Science Reviews*, v. 57, p. 299-399.

Hibbard, J., van Staal, C., Rankin, D., and Williams, H., 2006. *Geology, lithotectonic map of the Appalachian Orogen (South), Canada-United States of America*, Geological Survey of Canada, Map 02096A, scale 1:1500000.

Higgins, M.W., 1966, *The geology of the Brevard lineament near Atlanta, Georgia*, Georgia Geological Survey, Bulletin 77, 49 p.

Higgins, M.W., Pickering, S.M., Jr., and Atkins, R.L., 1980, The Soapstone Ridge complex, Atlanta, Georgia; a transported mafic-ultramafic complex in the southeastern Appalachian piedmont (abs.), *Geological Society of America Abstracts with Programs*, v. 17, no. 2, p. 96.

Higgins, M.W. and Atkins, R.L., 1981, The stratigraphy of the Piedmont southeast of the Brevard Zone in the Atlanta, Georgia, area, in: Wigley, P.B. (ed), *Latest thinking on the stratigraphy of selected areas in Georgia*, Georgia Geologic Survey Information Circular 54-A, p. 3-40.

Higgins, M.W., Atkins, R.L., Crawford, T.J., Crawford, R.F., III and Cook, R.B., 1984, A brief excursion through two thrust stacks that comprise most of the crystalline terrane of Georgia and Alabama, *Georgia Geological Society*, Guidebook, 9th Annual Field trip, 67 p.

Higgins, M.W., Atkins, R.L., Crawford, T.J., Crawford, R.F., III, Brooks, R. and Cook, R.B., 1988, The structure, stratigraphy, tectonostratigraphy, and evolution of the southernmost part of the Appalachian orogen, *U.S. Geological Survey Professional Paper*, 1475, 173 p.

Higgins, M.W. and Crawford, R.F., 2007, *Geologic map of the Atlanta 30-minute x 60-minute quadrangle, Georgia*, The Geologic Mapping Institute, Clayton, Georgia.

Hooper, R.J., and Hatcher, R.J., Jr., 1989, The origin of ultramafic rocks from the Bernermafic complex, central Georgia, In: S.K. Mittwede and E.F. Stoddard (eds.), *Ultramafic rocks of the Appalachian Piedmont*, Geological Society of America, Special Paper 231, p. 87-92.

Hopkins, O.B., 1914, *A report on the asbestos, talc and soapstone deposits of Georgia*, Geological Survey of Georgia, Bulletin no. 29, 319 p.

Jaques, A.L., Chappell, B.W. and Taylor, S.R., 1983, Geochemistry of cumulus peridotites and gabbros from the Marum ophiolite complex, northern Papua New Guinea, *Contributions to Mineralogy and Petrology*, v. 82, p. 154-164.

Kite, L.E. and Stoddard, E.F., 1984, The Halifax County complex: oceanic lithosphere in the eastern North Carolina Piedmont, *Geological Society of America Bulletin*, v. 95, p. 422-432.

Larrabee, D.M., 1966, Map showing distribution of ultramafic and intrusive mafic rocks from northern New Jersey to eastern Alabama, US Geological Survey Map, I-476.

La Tour, T.E., 1987, Analyses of rocks using X-Ray fluorescence spectrometry, *Rigaku Journal*, v. 6, p. 3-9.

Maier, W.D., Arndt, N.T. & Curl, E.A., 2000, Progressive

crustal contamination of the Bushveld Complex: evidence from Nd isotope analyses of the cumulate rocks, *Contributions to Mineralogy and Petrology*, v. 140, p. 316-227.

Mathison, C.I. & Hamlyn, P.R., 1987, The McIntosh layered troctolite-olivine gabbro intrusion, East Kimberley, Western Australia, *Journal of Petrology*, v. 28, 211-234.

Misra, K.C. and Keller, F.B., 1978, Ultramafic bodies in the southern Appalachians: a review, *American Journal of Science*, v. 278, p. 389-418.

Misra, K.C. and McSween, H.Y., 1984, Mafic and ultramafic rocks of the Appalachian orogeny – an introduction, *American Journal of Science*, v. 284, p. 290-293.

Niu, Y. and O'Hara, M.J., 2008, Global correlations of ocean ridge basalt chemistry with axial depth: a new perspective, *Journal of Petrology*, v. 49, p. 633-664.

Norrish, K. and Hutton, J.T., 1969, An accurate x-ray spectrographic method for the analyses of a wide range of geological samples, *Geochimica et Cosmochimica Acta*, v. 33, p. 431-453.

Owens, B.E. and Uschner, N.E., 2001, Mineralogy and geochemistry of metamorphosed ultramafic rocks in the central Piedmont Province of Virginia, *Southeastern Geology*, v. 40, p. 213-229.

Paster, T.P., Schauwecker, D.S. and Haskin, L.A., 1974, The behaviour of some trace elements during the solidification of the Skaergaard layered series, *Geochimica et Cosmochimica Acta*, v. 38, p. 1549-1577.

Pearce, J.A. and Norry, M.J., 1979, Petrogenetic implications of Ti, Zr, Y, and Ni variations in volcanic rocks, *Contributions to Mineralogy and Petrology*, v. 69, p. 33-47.

Peterson, V. and Ryan, J.G., 2009, Petrogenesis and structure of the Buck Creek mafic-ultramafic suite, southern Appalachians: constrains on ophiolite evolution and emplacement in collisional orogens, Geological Society of America Bulletin, v. 121, p. 615-629.

Philpotts, A.R., 1990, *Principles of igneous and metamorphic petrology*, Prentice Hall, Englewood Cliffs, NW, 498 p.

Pickering, S.M. and Schneeberger, F.J., III, 1972, General geology of the Soapstone Ridge mafic intrusive area, *Georgia Academy of Science Bulletin 30*, p. 78-79.

Pratt, J.H., and Lewis, J.V., 1905, *Corundum and the peridotites of North Carolina*, North Carolina Geological Survey, v. 1, 464 p.

Rioux, M., Hacker, B., Mattinson, J., Kelemen, P., Blusztajn, J. and Gehrels, G, 2007, Magmatic development of an intra-oceanic arc: high precision zircon and whole-rock isotopic analyses from the accreted south-central Alaska, *Geological Society of America Bulletin*, v. 119, p. 1168-1184.

Rollinson, H.R., 1993, *Using geochemical data: evaluation, presentation, interpretation*, John Wiley and Sons, New York, 352 p.

Savov, I., Ryan, J., Haydoutov, I. and Schijf, J., 2001, Late Precambrian Balkan-Carpathian ophiolite – a slice of the Pan African ocean crust?: geochemical and tectonic insights from the Tcherni Vrah and Deli Jovan massifs, Bulgaria and Serbia, *Journal of Volcanology and Geothermal Research*, v. 110, p. 299-318.

Schilling, J-G., Zajac, M., Evans, R., Johnston, T, White, W., Devine, J.D. and Kingsley, R., 1983, Petrologic and geochemical variations along the Mid-Atlantic Ridge from 29°N to 73°N, *American Journal of Science*, v. 283, p. 510-586.

Schroeder, P.A., Melear, N.D., West, L.T. and Hamilton, D.E., 2000, Meta-gabbro weathering in the Georgia Piedmont, USA: implications for global silicate weathering rates, *Chemical Geology*, v. 163, p. 235-245.

Spandler, C.J., Arculus, R.J., Eggins, S.M., Mavrogenes, J.A., Price, R.C. and Reay, A.J., 2003, Petrogenesis of the Greenhills complex, Southland, New Zealand: magmatic differentiation and cumulate formation at the roots of a Permian island-arc volcano, *Contributions to Mineralogy and Petrology*, v. 144, p. 703-721.

Streckeisen, A., 1976, To each plutonic rock its proper name, *Earth Science Reviews*, v. 12, p. 1-33.

Thornber, C.R., Budahn, J.R., Ridley, W.I. and Unruh, D.M., 2003, Trace element and Nd, Sr, Pb isotope geochemistry of Kilauea volcano, Hawai'i, near-vent eruptive, *U.S. Geological Survey, Open File Report 03-493*, 5p.

Thornber, C.R., 2001, Olivine-liquid relations of lava erupted by Kilauea volcano from 1994 to 1998: implications for shallow magmatic processes associated with the ongoing East-Rift-Zone eruption, *Canadian Mineralogist*, v. 39, p. 239-266.

Warner, R.D., Griffin, V.S., Jr., Hoover, R.C., Bryan, J.G., Poe, S,H., and Steiner, J.C., 1986, Mineralogy of ultramafic-amphibole schists, Inner Piedmont belt, South Carolina, Southeastern Geology, v. 27, p. 107-120.

Warner, R.D., Griffin, V.S., Steiner, J.C., Schmitt, R.A. and Bryan, J.G., 1989, Ultramafic chlorite-tremolite-olivine schists: three bodies from the Inner Piedmont belt, South Carolina, in: S.K. Mittwede and E.F. Stoddard (eds), *Ultramafic Rocks of the Appalachian Piedmont*, Geological Society of America, Special Paper 231, p. 63-74.

West, H.B., Garcia, M.O., Gerlach, D.C. and Romano, J., 1992, Geochemistry of tholeiites from Lanai, Hawaii, *Contributions to Mineralogy and Petrology*, v. 112, p. 520-542.

Wilson, M., 1989, Igneous petrogenesis – a global tectonic approach, Kluwer Academic Publishers, Dordrecht, 466 p.

Winter, J.D., 2010, *An introduction to igneous and metamorphic petrology*, Prentice Hall, Upper Saddle River, New Jersey, 697 p.ers, 2003).

SOUTHEASTERN GEOLOGY
V. 48, No. 4, February 2012, p. 207-212

A POST-HURRICANE IVAN BEACH-EROSION ASSESSMENT FROM A LOCATION ALONG ORANGE BEACH, ALABAMA (U.S.A.)

CARL R. FROEDE JR.

United States Environmental Protection Agency
Region 4
61 Forsyth Street, S.W.
Atlanta, GA 30303-8960

ABSTRACT

Hurricane Ivan's intensive wind fields, located just outside the northeastern quadrant of its eyewall, added to the storm surge and erosive force of storm waves as the hurricane made landfall just west of Gulf Shores, Alabama, shortly before 2:00 a.m. (CDT) on September 16, 2004. The upper Category 3 hurricane (Saffir–Simpson scale) generated a storm surge as high as 4.6 m above mean sea level along the shoreline of Baldwin County, Alabama. The United States Geological Survey conducted an aerial photographic assessment of sections of Orange Beach, both before and following Hurricane Ivan. The images documented post-hurricane beach erosion and the destruction of beachfront property along this section of the Alabama coast. A ground-based assessment examined one of the photographed post-hurricane locations along Orange Beach to ascertain the cause of damage to the beachfront property. It was determined that the storm surge and erosive storm waves combined to remove a significant volume of beach sand. Much of the property damage was due to the undermining of many residential structures within the foredune complex despite their distance from the former shoreline.

INTRODUCTION

The landfall of a hurricane in the northern Gulf of Mexico is typically marked by varying degrees of coastal erosion as a function of its speed over water and its storm surge. Larger, slower moving tropical storms can create an elevated storm surge and erosive storm waves that can rapidly erode a coastline. Hurricane Ivan adversely impacted the eastern Alabama and western Florida Panhandle coastlines in this manner (United States Geological Survey, 2004; Douglass and others, 2004; Douglass and Browder, 2005; Froede, 2006; Stewart, 2006; Wang and others, 2006; Houser and others, 2007; Morton, 2007; Houser, 2009). The United States Geological Survey conducted an aerial photographic assessment of portions of Orange Beach, Alabama, both before and following Hurricane Ivan. The post-hurricane images reveal significant beach erosion and property loss at some distance from the shoreline. A ground-based assessment was conducted at one of the photographed locations along Orange Beach to determine the cause of the damage to the beachfront residential property.

HURRICANE IVAN

Hurricane Ivan was a powerful hurricane (Figure 1). Winds at landfall averaged 209 km/hr with a storm surge along the eastern Alabama and western Florida panhandle coastlines ranging from 4.6 m to 3.0 m, respectively (Medlin and others, 2004; Stewart, 2006). The large storm made landfall as an upper Category 3 hurricane (Saffir-Simpson scale) just west of Gulf Shores, Alabama, at approximately 0650 UTC, on September 16, 2004 (Figure 2). According to Stewart (2006):

> There was a robust and persistent velocity maximum located within vigorous convection in the northeastern quadrant of the outermost concentric eyewall as Ivan was coming ashore. For several hours prior to landfall, the velocities

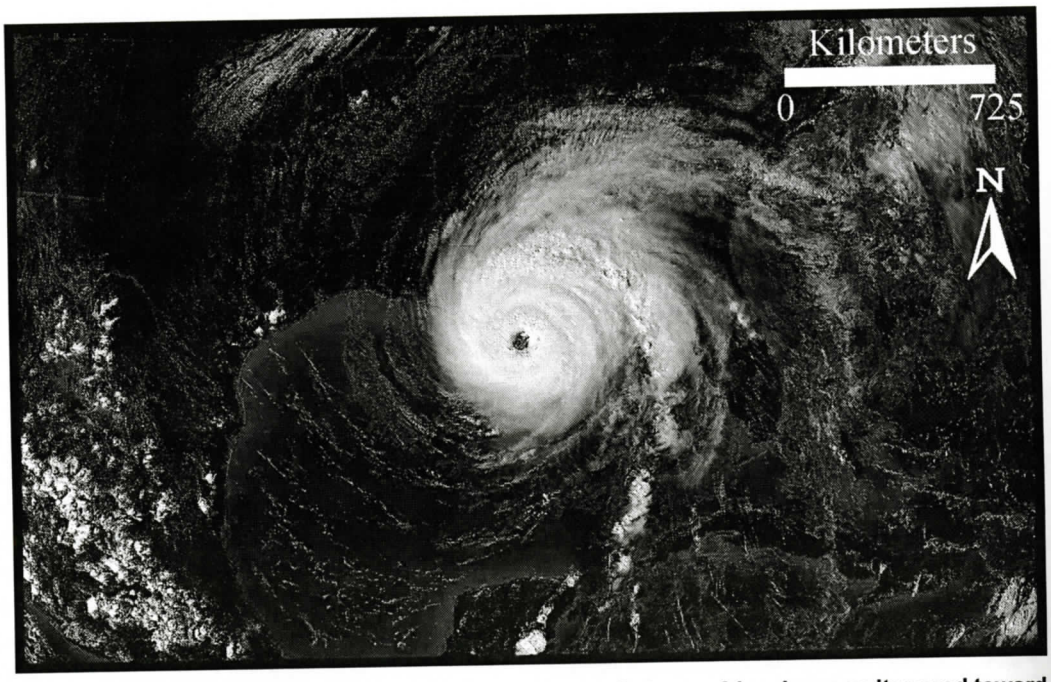

Figure 1. Hurricane Ivan was a large and powerful upper Category 3 hurricane as it moved toward the Alabama coastline. This satellite image was taken at 3:15 p.m. (CDT) on September 15, 2004, just hours before making landfall. Image courtesy of the National Oceanic and Atmospheric Administration.

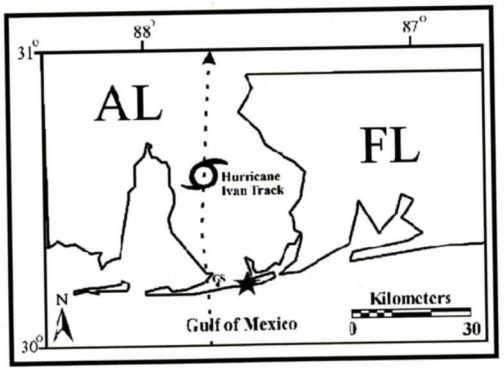

Figure 2. Hurricane Ivan passed to the west of Gulf Shores, Alabama (GS), as it made landfall early in the morning of September 16, 2004. This powerful storm damaged or destroyed considerable beachfront property along the eastern Alabama and western Florida Panhandle coastlines. The star indicates the location of the study area at Orange Beach, Alabama.

were actually higher in this area than in the vicinity of the inner eyewall.

This area of intensive wind energy occurred offshore from Orange Beach, Alabama, and likely contributed to large storm waves and an elevated storm surge along this section of the Alabama beach as it made landfall.

SIGNIFICANT BEACH EROSION AT ORANGE BEACH

The United States Geological Survey periodically conducts an aerial photographic survey of the coastline for those States located adjacent to the Gulf of Mexico. Much of this work has highlighted shoreline changes and property damage following tropical storms. Sections of Orange Beach were photographed before and following Hurricane Ivan. One set of aerial images from a location along Orange Beach show a small condominium and a beach house before (Figure 3a) and following (Figure 3b) the passing of Hurricane Ivan. The post-Ivan image indicates that both structures have been damaged or destroyed, but the exact cause (i.e., wind or water) is unknown.

A ground based survey of this same area revealed that the structural collapse of the small

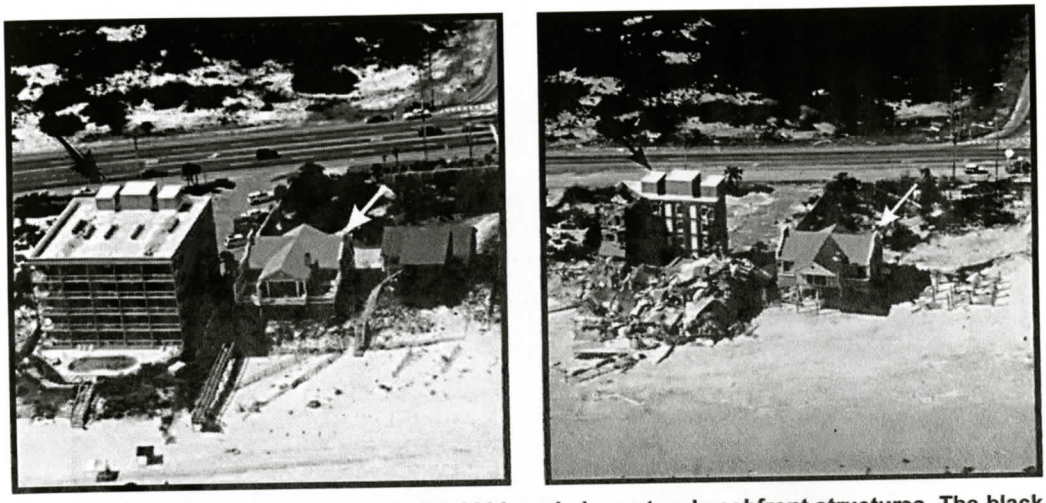

Figure 3. A. Aerial image is from July 17, 2001, and shows two beachfront structures. The black arrow points to a small-scale condominium and the white arrow points to a beach house. Approximate coordinates: N 30.2689 – W 87.5864. Image courtesy of the U.S. Geological Survey, Center for Coastal and Watershed Studies. B. Aerial image is from September 17, 2004, and shows damage experienced by the two structures from Hurricane Ivan. Viewed from this distance, the exact cause of the damage (i.e., wind or water) is uncertain. Image courtesy of the U.S. Geological Survey, Center for Coastal and Watershed Studies.

condominium and erosion of sand beneath the beach house was not due to the storm's high winds, but rather from the erosion caused by Ivan's large storm surge and erosive storm waves. Although developed for barrier islands, this level of coastal erosion is consistent with "Impact Level 2" based on the storm impact scale proposed by Sallenger (2000, p. 894):

Impact Level 2 - Collision Regime

1) Runup collides with the base of the foredune ridge.
2) The collision forces sand to be eroded from the dune and transported offshore.
3) Eroded sand is not readily returned to the dune, hence there is net erosion.

Many buildings constructed on pilings or stilts along the former shore-parallel foredune complex reveal the extent of storm erosion by their painted posts. Following Ivan, the underlying, unpainted sections of those posts document the volume of sand lost during the storm (Figure 4). The collapsed condominiums appear to have been constructed on unsupported cement slabs that were undermined by the elevated storm surge and erosive storm waves. Once sand was removed from beneath a portion of the foundation, the buildings simply collapsed due to structural instability. This erosional process was also noted by Stewart (2006) for many structures adjacent to the former surf zone along Orange Beach:

> ...extensive beach erosion caused severe damage to or the destruction of numerous beachfront homes, as well as apartment and condominium buildings. Some buildings collapsed due to scouring of the sand from underneath the foundations caused by the inundating wave action.

Douglass and Browder (2005, p. 73) conducted a post-Ivan damage assessment along sections of Orange Beach and they determined:

> Post-storm surveys reveal sand losses along the upper beach of 25-40 cy/ft and vertical scour of the beach up to 10 feet or more. ...The erosion of the upper beach extended well landward of the seaward edge of construction, destroying individual homes, exposing pilings and pile caps, stranding swimming pools, and in several notable instances causing the collapse of multi-story slab-

Figure 4. This photograph of the two structures shown in Figures 3a and 3b reveals that considerable beach sand has been removed by Hurricane Ivan's storm surge and erosive storm waves. The painted wooden stilts indicate the former elevation of beach sand beneath the house. The unpainted portion of the stilts at the front of the house is approximately 2.4 m above the ground surface. The adjacent small condominium was constructed on an unsupported concrete slab that was undermined during the course of the storm by the elevated storm surge and storm waves. Image from November 2004.

Figure 5. A large section of the coastline at Orange Beach has been flattened by Hurricane Ivan's storm surge and erosive storm waves. This was the state of the shoreline and beach on November 2004. View looking west.

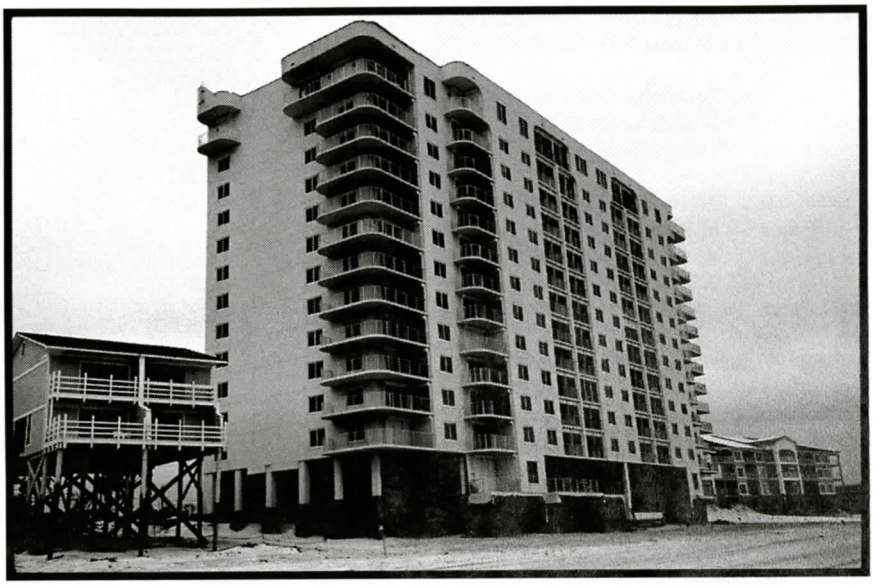

Figure 6. This large condominium was constructed on deeply driven concrete pilings which allowed it to withstand Ivan's storm surge, storm waves, and the loss of beach sand from in front of and beneath the building. Image from November 2004.

foundation-supported condominiums.

SUMMARY AND CONCLUSIONS

Hurricane Ivan was a large and powerful tropical storm that impacted the eastern Alabama and western Florida Panhandle coastlines with upper Category 3 winds and an exceptionally high storm surge. While it did not linger in its landfall just west of Gulf Shores, Alabama, the combination of the large storm surge and erosive storm waves removed a significant volume of sand from the Orange Beach coastline. The resulting beach was planed down to a relatively flat surface (Figure 5). Residential buildings normally considered to be a safe distance from the surf zone were suddenly inundated by elevated, erosive storm waves.

The storm surge and erosive storm waves reached farther landward than building codes had likely estimated. Structures constructed with slab foundations collapsed when undermined, while buildings with deep foundations only suffered the loss of surrounding beach sand (Figure 6).

The results of this investigation indicate that Ivan's large storm surge and erosive storm waves combined to remove a significant volume of beach sand within the study area (see also Douglass and Browder, 2005). Many of the beach houses and small condominiums that were along the gulf-facing foredune complex and relatively distant from the original shoreline were undermined by erosive storm waves, resulting in the partial or total collapse of those structures.

ACKNOWLEDGMENTS

I am grateful to A.J. Akridge, J.K. Reed and the anonymous reviewers for their constructive review and comments. This work neither represents the views or opinions of the U.S. Environmental Protection Agency or the United States, nor was this investigation conducted in any official capacity. Any mistakes are my own responsibility.

REFERENCES CITED

Douglass, S.L., Hughes, S., Rogers, S., and Chen, Q., 2004. The Impact of Hurricane Ivan to the Coastal Roads in Florida and Alabama: A Preliminary Report: Mobile, Alabama, University of South Alabama, Coastal Transportation Engineering Researchand Education Center.

Douglass, S.L., and Browder, A.E., 2005. Hurricane Ivan's impacts on the Alabama coast: Shore and Beach, v. 73, p. 71-78.

Froede, C.R., Jr., 2006. The impact that Hurricane Ivan (September 16, 2004) made across Dauphin Island, Alabama: Journal of Coastal Research, v. 22, p. 561-573.

Houser, C., Hamilton, S., Meyer-Arendt, K., and Oravetz, J., 2007. EOF analysis of barrier island morphological change during Hurricane Ivan, *in* Kraus, N.C., and Rosati, J.D., eds., Proceedings of Coastal Sediments'07: Reston, VA, American Society of Civil Engineers, p. 986–995.

Houser, C., 2009. Geomorphological Controls on Road Damage during Hurricanes Ivan and Dennis: Journal of Coastal Research, v. 25, p. 558–568.

Medlin, J., Ball, R., and Beeler, G., 2004. Powerful Hurricane Ivan slams the U.S. central Gulf Coast as an upper Category 3 storm. Accessed from: http://www.srh.noaa.gov/mob/ivan_page/Ivan-main.htm.

Morton, R.A., 2007. Historical changes in the Mississippi-Alabama barrier islands and the roles of extensive storms, sea level, and human activities. U.S. Geological Survey Open File Report 2007-1161. Accessed from: http://pubs.usgs.gov/of/2007/1161/.

Sallenger, A.H., Jr., 2000. Storm impact scale for barrier islands: Journal of Coastal Research, v. 16, p. 890-895.

Stewart, S.R., 2006. Hurricane Ivan tropical cyclone report. Accessed from: http://www.nhc.noaa.gov/2004ivan.shtml?.

United States Geological Survey, 2004. Hurricane Ivan impact studies. Accessed from: http://coastal.er.usgs.gov/hurricanes/ivan/.

Wang, P., Kirby, J.H., Haber, J.D., Horwitz, M.H., Knorr, P.O., and Krock, J.R., 2006. Morphological and sedimentological impacts of Hurricane Ivan and immediate poststorm beach recovery along the northwestern Florida barrier-island coasts: Journal of Coastal Research, v. 22, p. 1382-1402.

SOUTHEASTERN GEOLOGY
Duke University
Box 90233
Durham, NC 27708-0233

Returned Service Requested

Non-Profit Org.
U. S. POSTAGE
P A I D
Durham, NC
Permit No. 60

BELK LIBRARY
SERIALS DEPT
APPALACHIAN STATE UNIVERSITY
PO BOX 32026
Boone, NC 28608